CORA Cork Open Research Archive
Cartlann Taighde Oscailte Chorcaí

Title	Synthesis and evaluation of aromatic BDSF bioisosteres on biofilm formation and colistin sensitivity in pathogenic bacteria
Authors	Gómez, Andromeda-Celeste;Horgan, Conor;Yero, Daniel;Bravo, Marc;Daura, Xavier;O'Driscoll, Michelle;Gibert, Isidre;O'Sullivan, Timothy P.
Publication date	2023-09-23
Original Citation	Gómez, A.-C., Horgan, C., Yero, D., Bravo, M., Daura, X., O'Driscoll, M., Gibert, I. and O'Sullivan, T.P. (2023) 'Synthesis and evaluation of aromatic BDSF bioisosteres on biofilm formation and colistin sensitivity in pathogenic bacteria', European Journal of Medicinal Chemistry, 261, 115819 (16 pp). https://doi.org/10.1016/j.ejmech.2023.115819.
Type of publication	Article (peer-reviewed)
Link to publisher's version	https://doi.org/10.1016/j.ejmech.2023.115819 - 10.1016/j.ejmech.2023.115819
Rights	© 2023 The Authors. Published by Elsevier Masson SAS. This is an open access article under the CC BY license (http://creativecommons.org/licenses/by/4.0/). - http://creativecommons.org/licenses/by/4.0/
Download date	2026-11-10 09:19:57
Item downloaded from	https://hdl.handle.net/10468/15122

UCC
University College Cork, Ireland
Coláiste na hOllscoile Corcaigh

European Journal of Medicinal Chemistry 261 (2023) 115819

Contents lists available at ScienceDirect

European Journal of Medicinal Chemistry

journal homepage: www.elsevier.com/locate/ejmech

Research paper

Synthesis and evaluation of aromatic BDSF bioisosteres on biofilm formation and colistin sensitivity in pathogenic bacteria

Andromeda-Celeste Gómez [a,b,1], Conor Horgan [c,1], Daniel Yero [a,b], Marc Bravo [a,b], Xavier Daura [a,d,e], Michelle O'Driscoll [c,f,g], Isidre Gibert [a,b,**], Timothy P. O'Sullivan [c,f,g,*]

[a] Institut de Biotecnologia i de Biomedicina, Universitat Autònoma de Barcelona, Barcelona, Spain
[b] Departament de Genètica i de Microbiologia, Universitat Autònoma de Barcelona, Barcelona, Spain
[c] School of Chemistry, University College Cork, Cork, Ireland
[d] Catalan Institution for Research and Advanced Studies (ICREA), Barcelona, Spain
[e] CIBER de Bioingeniería, Biomateriales y Nanomedicina, Instituto de Salud Carlos III, Cerdanyola de Vallès, Spain
[f] School of Pharmacy, University College Cork, Cork, Ireland
[g] Analytical and Biological Chemistry Research Facility, University College Cork, Cork, Ireland

ARTICLE INFO

Keywords:
Diffusible signal factor
Quorum sensing
Biofilms
Resistance
Acinetobacter baumannii
Escherichia coli
Burkholderia multivorans
Burkholderia cepacia
Burkholderia cenocepacia
Pseudomonas aeruginosa and Stenotrophomonas maltophilia

ABSTRACT

The diffusible signal factor family (DSF) of molecules play an important role in regulating intercellular communication, or quorum sensing, in several disease-causing bacteria. These messenger molecules, which are comprised of *cis*-unsaturated fatty acids, are involved in the regulation of biofilm formation, antibiotic tolerance, virulence and the control of bacterial resistance. We have previously demonstrated how olefinic *N*-acyl sulfonamide bioisosteric analogues of diffusible signal factor can reduce biofilm formation or enhance antibiotic sensitivity in a number of bacterial strains. This work describes the design and synthesis of a second generation of aromatic *N*-acyl sulfonamide bioisosteres. The impact of these compounds on biofilm production in *Acinetobacter baumannii*, *Escherichia coli*, *Burkholderia multivorans*, *Burkholderia cepacia*, *Burkholderia cenocepacia*, *Pseudomonas aeruginosa* and *Stenotrophomonas maltophilia* is evaluated, in addition to their effects on antibiotic tolerance. The ability of these molecules to increase survival rates on co-administration with colistin is also investigated using the *Galleria* infection model.

1. Introduction

Diffusible signal factor (DSF) is one of an important family of quorum sensing (QS) signalling molecules found in Gram negative bacteria [1]. DSF (**1**) was first identified in *Xanthomonas campestris pv campestris* (*Xcc*), the bacterium responsible for black rot, a major disease of cruciferous plants (Fig. 1) [2]. *Xcc* contains a cluster of genes, known as regulation of pathogenicity factors (*rpf*), which are essential for the synthesis of enzymes and extracellular polysaccharides [3]. Mutation of one of these genes results in activity failure in related enzymes. Daniels and co-workers demonstrated that the phenotype of an *rpfF* mutant could be corrected when cultivated in proximity to its wild-type parental strain [4]. It was postulated that a signalling molecule was responsible for this restoration and that the *rpfB* and *rpfF* genes played some part in its biosynthesis. The *rpfF* gene likely encodes an enoyl-coenzyme A (CoA) hydratase while the *rpfB* gene probably encodes a long chain fatty acyl CoA ligase. The structure of DSF was eventually confirmed to be the α,β-unsaturated fatty acid, *cis*-11-methyl-2-dodecenoic acid (**1**) [5].

Subsequently, a homologue of DSF from *B. cenocepacia* was isolated by Boon and colleagues, called BDSF (**2**) [6]. *B. cenocepacia* is a key bacterium in the *Burkholderia cepacia* complex (BCC) and is an opportunistic pathogen commonly found in immunocompromised individuals, including those with cystic fibrosis (CF) [7]. The key structural difference between the two molecules is the absence of the methyl group at C-11 in BDSF. It was later established that BDSF can also inhibit the ability of *Candida albicans* to switch between yeast and hyphal forms [6,8]. In recent years, several additional species of bacteria have been found to employ members of the DSF family in their quorum

* Corresponding author. School of Chemistry, University College Cork, Cork, Ireland.
** Corresponding author. Institut de Biotecnologia i de Biomedicina, Universitat Autònoma de Barcelona, Barcelona, Spain.
E-mail addresses: Isidre.Gibert@uab.cat (I. Gibert), Tim.OSullivan@ucc.ie (T.P. O'Sullivan).
[1] These authors contributed equally.

https://doi.org/10.1016/j.ejmech.2023.115819
Received 14 August 2023; Received in revised form 11 September 2023; Accepted 12 September 2023
Available online 15 September 2023
0223-5234/© 2023 The Authors. Published by Elsevier Masson SAS. This is an open access article under the CC BY license (http://creativecommons.org/licenses/by/4.0/).

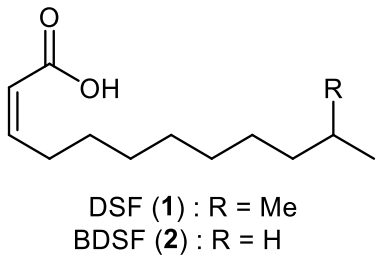


Fig. 1. Structures of DSF and BDSF signalling molecules.

sensing systems including *Pseudomonas* sp. [9], *Stenotrophomonas maltophilia* (*Sm*) [10], *Xanthamonas oryzae* [11] and *Xylella fastidiosa* [12].

Wang and co-workers investigated the effects of a library of DSF derivatives on *Xcc* virulence in order to determine the structural features that were important for biological activity [5]. A key finding was that the location and configuration of the double bond was important for activity. For example, the saturated fatty acid 11-methyldodecanoic acid was 20,000-fold less active in the induction of virulence gene expression than DSF. Additionally, *cis*-unsaturated DSF was 200-fold more active than its *trans* isomer (i.e. *trans*-11-methyl-2-dodecenoic acid). The *cis*--configuration is likewise important in other DSF-sensitive pathogens including BCC, *Pseudomonas aeruginosa*, *C. albicans*, *Escherichia coli*, *Klebsiella pneumoniae*, *Proteus mirabilis*, *Streptococcus pyogenes*, *Bacillus subtilis*, and *Streptococcus mutans* [1,13,14]. A similar pattern was observed for BDSF – *trans*-BDSF, or *trans*-2-dodecenoic acid, was 33-fold less active than BDSF in *Xcc* while saturated dodecanoic acid was 333 times less effective than BDSF. Shortening or increasing the fatty acid chain length was also found to be detrimental.

In our search for novel quorum sensing inhibitors of DSF and BDSF, we previously synthesised a series of bioisosteres where the original carboxylic acid was replaced with an *N*-acyl sulfonamide group [15,16]. There is ample literature precedent to support the use of sulfonamides as bioisosteric equivalents of carboxylic acids [17–19]. Each of these 'olefinic sulfonamides' retained the *cis*-unsaturated double bond characteristic of the DSF family (Fig. 2). These molecules were found to possess anti-biofilm and anti-quorum sensing activity in *S. maltophilia*, BCC and *P. aeruginosa*. DSF production in *S. maltophilia* was also inhibited. The olefinic *N*-acyl sulfonamides not only reduced the minimal inhibitory concentration (MIC) of colistin in *Sm*-resistant isolates but also increased the larval survival of infected *Galleria mellonella* when co-administered with colistin.

One of the problems encountered in the synthesis of our olefinic *N*-acyl sulfonamide analogues was the tendency for the *cis*-alkene to isomerise to the thermodynamically favoured *trans*-isomer [20]. This behaviour is not uncommon, and many *cis*-unsaturated fatty acids readily isomerise due to the relatively low energy barrier between the *cis*- and *trans*-isomers [21]. We considered modifications to the structure that would allow us to essentially lock the double bond into the *cis*--configuration and thus prevent isomerisation. The incorporation of an aromatic ring at the C-2 position was proposed as a possible stable derivative of BDSF (Fig. 2). A similar approach has been exploited for lipoxin and resolvin analogues where a triene motif is replaced with a stable aromatic ring [22,23]. These 'aromatic sulfonamide' derivatives

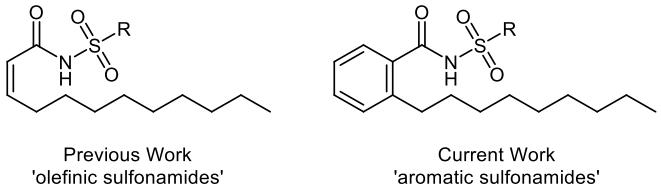


Fig. 2. Previous vs current work.

of BDSF retain twelve carbons in their backbone.

This article describes the preparation of a library of aromatic *N*-acyl sulfonamide derivatives of BDSF. The individual sulfonamides are evaluated for their inhibitory effects on biofilm production as well as their antimicrobial properties in nosocomial pathogens including *Acinetobacter baumannii*, *E. coli*, *B. multivorans*, *B. cepacia*, *B. cenocepacia*, *P. aeruginosa* and *S. maltophilia*. Additionally, the enhancing effects of the novel bioisosteres when co-administered with colistin are also reported.

2. Results and discussion

2.1. Chemistry

The preparation of the library of aromatic *N*-acyl sulfonamides revolved around carboxylic acid **7** (Fig. 3). As a common intermediate, **7** could be coupled with various sulfonamides to create a library of bioisosteric analogues. Starting from 2-iodobenzoic acid (**3**), methyl 2-iodobenzoate (**4**) was synthesised using standard Fisher esterification conditions by heating **3** and catalytic sulfuric acid in methanol to reflux to afford the methyl ester in 91% yield [24]. The next step was to introduce the alkyl chain *via* Pd/Cu-mediated Sonogashira coupling. Coupling of **4** and 1-nonyne using bis(triphenylphosphine)palladium(II) dichloride and copper (I) iodide as the catalyst system at room temperature did furnish the target **5**, albeit in a low yield of 22%. Increasing the temperature to reflux saw a modest improvement in yield to 27% after 24 h. The use of microwave irradiation in metal-catalysed reactions is often associated with higher yields and reduced reaction times [25–27]. When the reaction mixture was heated to 100 °C under microwave irradiation in anhydrous acetonitrile, alkyne **5** was recovered in a much improved yield of 66% yield. The copper acetylide species generated *in situ* can render Sonogashira reactions sensitive to air, with Glaser homocoupling of the terminal alkyne being the main undesired side reaction [28,29]. Repeating the reaction in degassed solvent saw full consumption of **4** after 60 min and elimination of the unwanted homocoupled by-product. Thereafter, target alkyne **5** could be consistently recovered in 88% yield under these optimised conditions. Alkyne **5** was reduced to corresponding alkane **6** *via* hydrogenation at atmospheric pressure after 16 h with a 10 mol% loading of palladium on carbon. Evidence for this transformation was provided by the shift of two signals at 79.2 ppm and 96.1 ppm to 34.5 ppm and 31.8 ppm respectively in the ^{13}C NMR spectrum of **6**. Halving the loading of the catalyst resulted in incomplete consumption of **5**, even with extended reaction times. By contrast, full conversion of **5** was again observed on replacing Pd/C with Adam's catalyst at the lower 5 mol% loading, with **6** obtained in quantitative yield. Methyl ester **6** was hydrolysed with lithium hydroxide in THF/methanol/water when heated to reflux over 16 h. Reacidification and concentration *in vacuo* provided 2-nonylbenzoic acid (**7**) as a pale-yellow oil in 94% yield without need of further purification. Formation of the carboxylic acid was confirmed by the appearance of a broad O–H stretch centred on 2923 cm^{-1} in the infra-red spectrum of **7**.

The next step was the preparation of the *N*-acyl sulfonamide derivatives for subsequent evaluation. A range of alkyl- and aryl-substituted sulfonamides were selected for coupling with **7** to generate a library with sufficient structural diversity. Taking *N*-(methanesulfonyl)-2-nonylbenzamide (**8**) as a typical example, methanesulfonamide was coupled with 2-nonyl benzoic acid (**7**) in the presence of 1.1 equivalents of DCC and DMAP in dichloromethane (Table 1, entry 1). Following work up and purification by silica gel column chromatography, *N*-acyl sulfonamide **8** was obtained as an off-white solid in 82% yield. A broad 1H singlet at 8.24 ppm representing the N–H signal was apparent in the ^{1}H NMR spectrum of **8**. A similar approach was employed for the remaining sulfonamides (entries 2–16) to create a library of 16 bioisosteres. The yields ranged from 31% (entry 16) to 96% (entry 13) with an average yield of 66%. The lowest yields

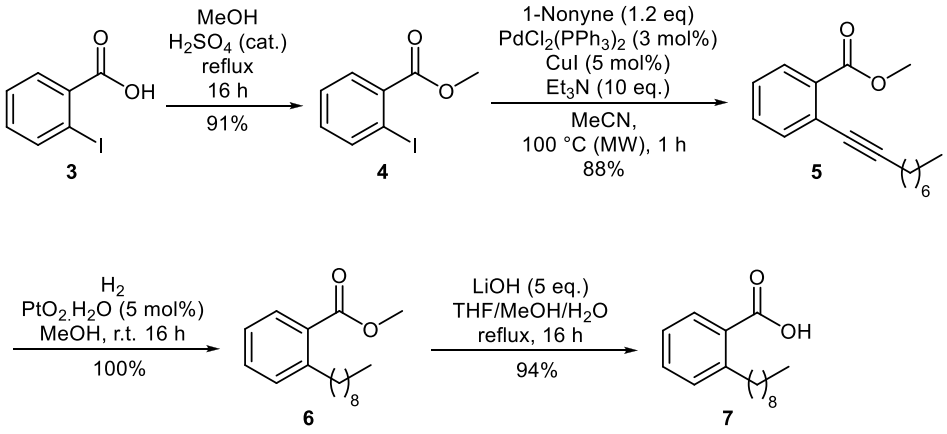
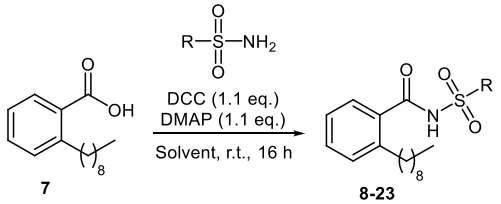


Fig. 3. Synthetic route to carboxylic acid intermediate 7.

Table 1
Preparation of aromatic *N*-acyl sulfonamides.



Entry	R	Solvent	Product	Yield
1	Me	DCM	**8**	82%
2	Cyclopropyl	DCM	**9**	58%
3	*t*Bu	DCM	**10**	73%
4	$CF_3(CH_2)_2$	DCM/DMF	**11**	36%
5	Ph	DCM	**12**	61%
6	2-BrC_6H_4	DCM	**13**	67%
7	3-BrC_6H_4	DCM	**14**	86%
8	4-BrC_6H_4	DCM	**15**	72%
9	2-FC_6H_4	DCM	**16**	66%
10	3-FC_6H_4	DCM	**17**	73%
11	4-FC_6H_4	DCM	**18**	57%
12	4-ClC_6H_4	DCM	**19**	64%
13	4-IC_6H_4	DCM	**20**	96%
14	4-*t*BuC_6H_4	DCM	**21**	69%
15	4-$MeOC_6H_4$	DCM	**22**	57%
16	4-$NO_2C_6H_4$	DCM/DMF	**23**	31%

were recorded for 3,3,3-trifluoropropanesulfonamide **11** (36%, entry 4) and 4-nitrobenzenesulfonamide **23** (31%, entry 16). For both reactions, the starting sulfonamides were not fully soluble in dichloromethane and required the addition of DMF as a co-solvent to improve solubility. In terms of structural diversity, the library could be split into alkyl- (entries 1–4) and aryl-substituted (entries 5–12) sulfonamides. Methyl analogue **8** (entry 1) was the simplest alkyl derivative. The cyclopropyl-containing sulfonamide (entry 2) is a privileged motif in medicinal chemistry which frequently appears in preclinical and clinical drug candidates, and thus warranted inclusion [30]. *tert*-Butyl analogue **10** (entry 3) provided more steric bulk while the 3,3,3-trifluoropropyl group (entry 4) appears in several pharmaceuticals and agrochemicals [31]. In addition to phenyl sulfonamide **12** (entry 5), a series of *ortho*-, *meta*- and *para*-brominated aryl sulfonamides (entries 6–8) was prepared. In our previous study, *ortho*-brominated analogues proved especially active. For comparsion, a number of similarly substituted fluorinated analogues (9-11) were included, along with *para*-substituted chlorine- (entry 12) and iodine-containing (entry 13) derivatives. To complete the library, electron rich analogues 4-*tert*-butylphenyl sulfonamide **21** (entry 14), 4-methoxyphenyl sulfonamide **22** (entry 15) and electron poor analogue 4-nitrophenyl sulfonamide **23** (entry 16) were also prepared.

2.2. Biological evaluation

2.2.1. Bacterial growth

Sixteen aromatic *N*-acyl sulfonamide analogues were tested against clinically relevant isolates of seven important nosocomial bacteria, namely *A. baumannii*, *E. coli*, *B. multivorans*, *B. cepacia, B. cenocepacia*, *P. aeruginosa* and *S. maltophilia*. BDSF (**1**) was also included in the assays as a reference compound. The *N*-acyl sulfonamides were tested for their intrinsic antimicrobial activity at 50 μM concentration (Fig. 4). None of the candidates displayed a significant growth inhibitory effect in *A. baumannii*, *E. coli* and *P. aeruginosa* (Supplementary Figure A1, A2 and A6). In *S. maltophilia*, both *meta*-bromophenylsulfonamide **14** and *para*-iodophenylsulfonamide **20** exhibited significant inhibitory activity, although the effect was much less pronounced in the case of **14** (Supplementary Figure A7). In *Burkholderia,* several of the compounds, in particular *para*-iodophenylsulfonamide **20**, were highly inhibitory with *B. multivorans* proving especially susceptible (Supplementary Figures A3, A4 and A5). These initial experiments suggest that any subsequent biological effects (e.g. reduced biofilm formation) observed in *A. baumannii* and *E. coli* in the presence of these molecules are likely due to disruption of intracellular communication rather than inhibition of bacterial growth.

2.3. Biofilm inhibition

The inhibitory effect of aromatic BDSF bioisosteres on biofilm formation in the seven bacterial strains was investigated on a polystyrene surface at 50 μM concentrations. A concentration of 50 μM was chosen as it is lies within the range at which natural BDSF or DSF typically exhibit physiological effects [32,33]. Additionally, this concentration allows for comparison with our prior work on olefinic BDSF analogues [15] or, more broadly, with halofuranone inhibitors of autoinducer-2 [34]. Bacterial biofilm formation in the presence of the compounds was compared with a control containing neat DMSO, which was benchmarked as 100% biofilm formation. Results were expressed as the average and standard deviation of duplicates of at least two independent experiments. Statistical significance was analysed by one-way ANOVA.

The impact on biofilm growth in *A. baumannii* was first investigated. *A. baumannii* is a leading nosocomial pathogen which exhibits high levels of virulence and is intrinsically resistant to many antimicrobials [35]. This biofilm-producing species of bacteria poses a significant threat, particularly in intensive care units [36,37]. The biofilms

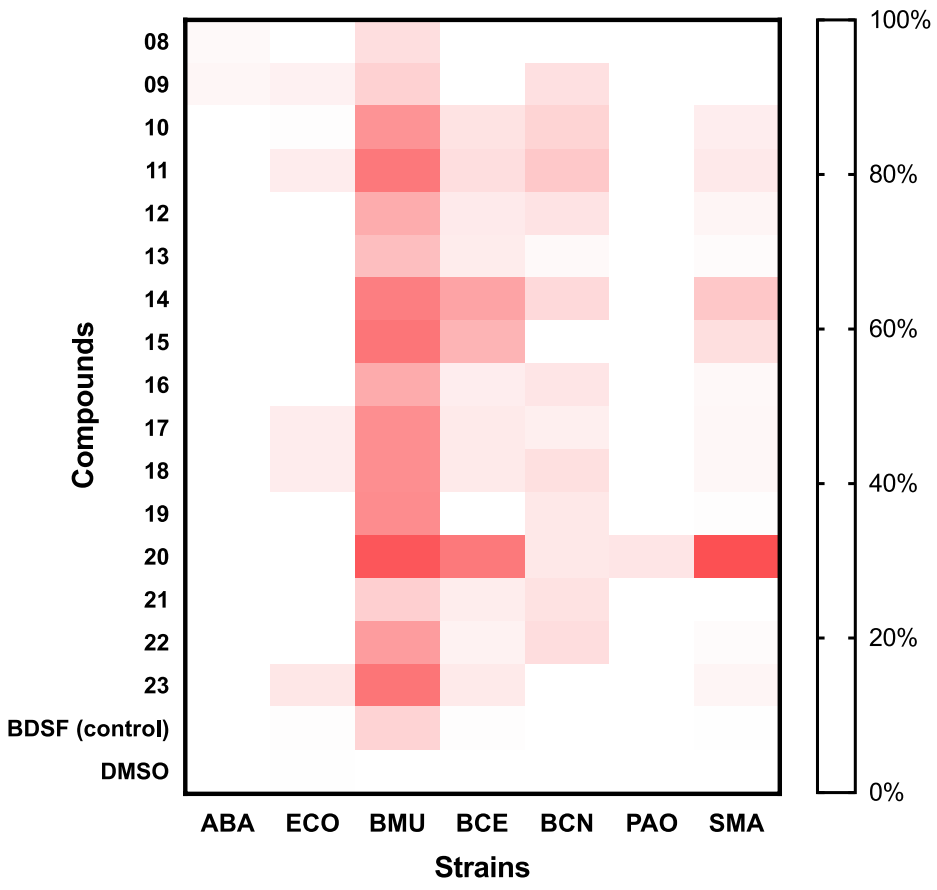


Fig. 4. Intrinsic inhibitory properties of aromatic sulfonamides. Heat map of mean growth inhibition values from at least two independent experiments for *A. baumannii* ATCC 15308 (ABA), *E. coli* ATCC 9637 (ECO), *B. multivorans* B10 (BMU), *B. cepacia* R6193 (BCE), *B. cenocepacia* 289 (BCN), *P. aeruginosa* PAO1 (PAO) and *S. maltophilia* K279a (SMA). The scale displays 0%–100% growth inhibition at 50 μM concentration of each sulfonamide. Control contains the same volume of neat DMSO.

produced by *A. baumannii* are maintained for the production of adhesins and capsular polysaccharides [38]. The strain used in this study was ATCC 15308. Most of our compounds inhibited biofilm growth to a statistically significant level with an average 26% inhibition recorded (Fig. 5). The most potent inhibitor was electron poor *para*--nitrophenylsulfonamide **23** which reduced biofilm formation by 50% (Fig. 6). Interestingly, the next most effective compound was electron rich *para*-methoxy analogue **22** which caused a 41% reduction. The substitution pattern was also found to be important. For example, *ortho*-bromophenylsulfonamide **13** (30% inhibition) was noticeably more active than *meta*-bromophenylsulfonamide **14** (1.5% inhibition) or *para*-bromophenylsulfonamide **15** (8% inhibition). The activity of *ortho*-, *meta*- and *para*-fluorophenylsulfonamides **16**–**18** was more consistent with inhibition values of 27%, 27% and 25% respectively, similar to **13**. Notably, the signalling molecule BDSF itself inhibited biofilm formation in the same strain by 38%. This behaviour has not been previously described in the literature. However, unsaturated fatty acids such as palmitoleic and myristoleic acid are reported to decrease biofilm formation in *A. baumannii* at 20 μg/mL concentrations [39].

E. coli is a Gram-negative pathogen which is responsible for roughly three quarters of all urinary tract infections [40]. The elevated ability of *E. coli* to form biofilms enhances its persistence making it difficult to treat. In hospital settings, these biofilms are frequently found on medical devices such as urethral and intravascular catheters, prosthetic joints, shunts and grafts [41]. BDSF is not known to affect biofilm formation in *E. coli* but it has been reported that the closely related *cis*-2-decenoic acid can induce dispersion of biofilms formed by *E. coli* [9]. *E. coli* ATCC 9637, a strain deemed safe for laboratory purposes, was selected as our test candidate [42]. *E. coli* ATCC 9637 proved quite susceptible to our aromatic analogues with the majority of compounds, apart from methylsulfonamide **8**, reducing biofilm formation to some extent (Fig. 7). By far the most potent inhibitors were halogenated analogues **14**, **15**, **19** and **20** each of which reduced biofilm formation by over 59% - a more pronounced effect than that observed in *A. baumannii*. These results suggest that a *para*- or *meta*-halogenated aryl sulfonamide could be an important structural feature for inhibition of biofilm growth in this species. The most active compound was *para*-iodophenylsulfonamide **20** which exhibited 68% biofilm inhibition. When the iodine atom was replaced by a bromine or chlorine, a comparable effect was recorded (i.e. 63% for **14** and 59% for **19**). Contrastingly, when the iodine was substituted with a fluorine atom, the inhibitory effect was appreciably reduced with 22% inhibition observed for **18**. *meta*--Bromophenylsulfonamide **14** caused a 63% reduction in biofilm formation whereas its *ortho*-brominated analogue **13** resulted in a 43% decrease, highlighting the sensitivity to substituent location. The structure activity relationships between our compound library and the different bacterial species proved to be highly variable. As a case in point, *para*-halogenated analogues **15**, **19** and **20**, which were among the most effective analogues for *E. coli* (Fig. 7), comprised the least effective inhibitors for *A. baumannii* (Fig. 6).

BCC is a group of closely related Gram-negative bacteria species that are involved in nosocomial infections and exhibit a high degree of antimicrobial resistance [43–45]. This complex includes not less than 20 bacterial species, including *B. multivorans*, *B. cepacia* and *B. cenocepacia*

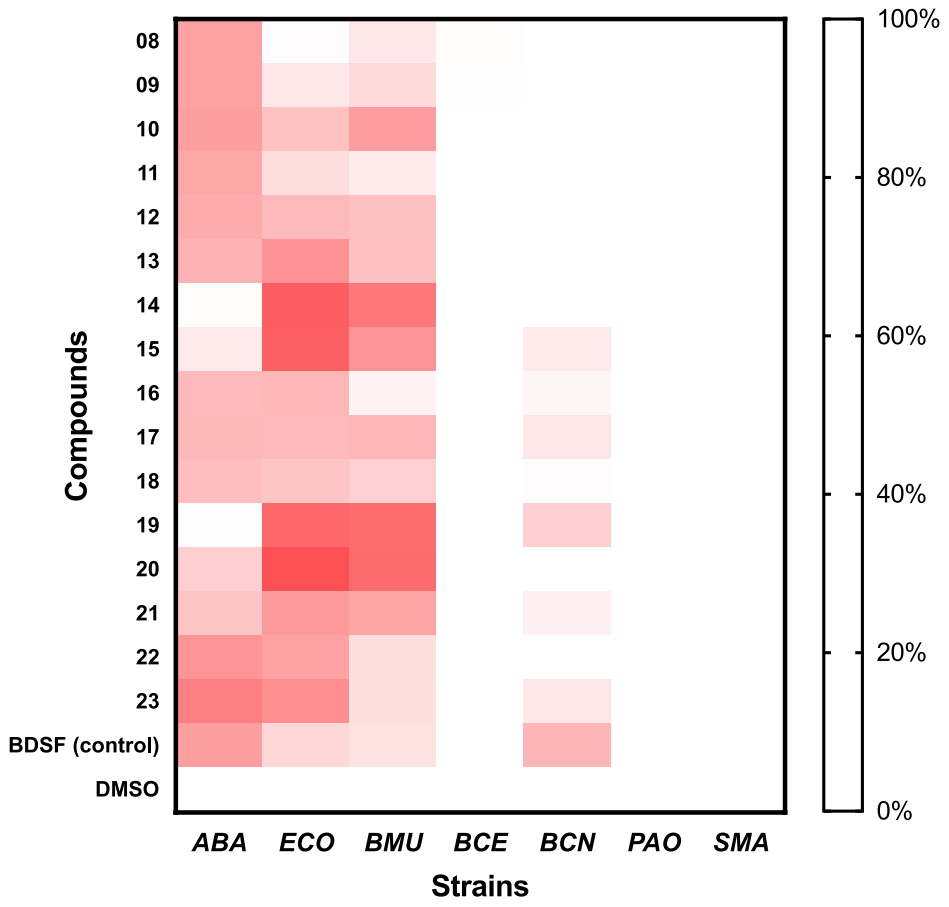


Fig. 5. Percentage biofilm inhibition by aromatic sulfonamides. Heat map of mean biofilm inhibition values from at least two independent experiments for *A. baumannii* ATCC 15308 (ABA), *E. coli* ATCC 9637 (ECO), *B. multivorans* B10 (BMU), *B. cepacia* R6193 (BCE), *B. cenocepacia* 289 (BCN), *P. aeruginosa* PAO1 (PAO) and *S. maltophilia* K279a (SMA). The scale displays 0%–100% biofilm inhibition at 50 μM concentration of each sulfonamide. Control contains the same volume of neat DMSO.

[46]. Members of BCC are known to form biofilms on biotic and abiotic surfaces, including medical devices [47]. As human pathogens, they are often associated with respiratory tract infections and are prevalent in patients with cystic fibrosis [48]. Bacterial behaviour, including virulence and biofilm formation, are regulated in BCC *via* BDSF-mediated quorum sensing [49]. In recent times, *B. multivorans* has overtaken *B. cenocepacia* as the most common BCC isolate in patients with CF in United States and the United Kingdom [50]. Accordingly, one of the clinical isolates investigated in this study was *B. multivorans* B10 [51]. Most of the 16 sulfonamides inhibited biofilm production in *B. multivorans* B10 (Fig. 8). This species of bacteria was most sensitive to *para*-chlorophenylsulfonamide **19** which reduced biofilm growth by 47% (Fig. 8). This was better than the corresponding *para*-bromophenylsulfonamide **15** (31% inhibition), *para*-fluorophenylsulfonamide **18** (27% inhibition), or *para*-iodophenylsulfonamide **20** (35% inhibition). The second most active molecule was *meta*-bromophenylsulfonamide **14** with 41% inhibition. *meta*-Bromophenylsulfonamide **14** outperformed its corresponding *ortho*- and *para*-brominated analogues **13** and **15** (38% and 31% inhibition respectively). Non-halogenated sulfonamides **10** and **21** were also highly active. Both structures contained a *tert*-butyl motif and inhibited biofilm formation by more than 35%.

By contrast, biofilm growth in the clinical strains *B. cepacia* R6193 (Fig. 9) and *B. cenocepacia* 289 (Fig. 10) was not significantly inhibited by the library of aromatic sulfonamides, highlighting the species-specific activity of the compounds tested. Indeed, *meta*-bromophenylsulfonamide **14** and *para*-bromophenylsulfonamide **15** appeared to promote biofilm production in *B. cepacia* R6193 (Fig. 9) while acting as biofilm inhibitors in *B. multivorans* B10 (Fig. 7).

P. aeruginosa is one of the most common biofilm-producing pathogens found in healthcare settings [52]. It is responsible for 10% of all nosocomial infections [36,37]. Often characterised by its high degree of virulence, *P. aeruginosa* is known to exhibit elevated levels of antimicrobial resistance (AMR) [35]. Although *P. aeruginosa* does not produce BDSF, it is capable of sensing the signalling molecule, resulting in the suppression of biofilm formation and virulence factor production [53]. The strain of *P. aeruginosa* employed in this study was PAO1 [54]. Biofilm formation in *P. aeruginosa* was not affected by any of the compounds in this library (Fig. 11). Instead, the *N*-acyl sulfonamides appeared to enhance biofilm growth with >100% normalised biofilm observed for all compounds.

S. maltophilia is a Gram-negative, nosocomial pathogen associated with pneumonia, bacteremia, UTIs and septic arthritis in immunocompromised patients [44,55]. Its prominent biofilm producing capabilities make *S. maltophilia* highly resistant to antimicrobials [43]. DSF is the main QS signalling molecule used by this pathogen to regulate biofilm formation and virulence [56]. The clinical isolate *S. maltophilia* K279a (belonging to the rpf-1 subpopulation) was used in the study. None of our aromatic sulfonamides inhibited biofilm formation and apparently caused increased biofilm growth compared to the DMSO control (Fig. 12). This result was unsurprising as we had previously observed a similar outcome with our olefinic sulfonamides [15].

As a general trend, aromatic *N*-acyl sulfonamides which contained a halogen group were found to be among the most effective inhibitors of

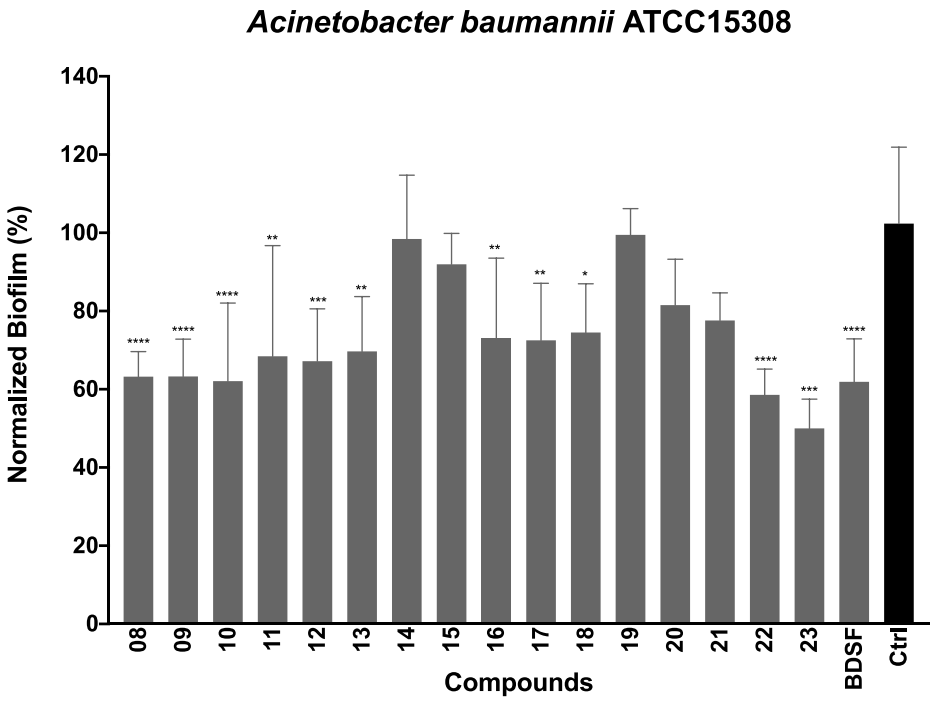


Fig. 6. Effect of sulfonamides on biofilm formation of *A. baumannii* ATCC15308 (*p < 0.05, **p < 0.01, ***p < 0.001, ****p < 0.0001).

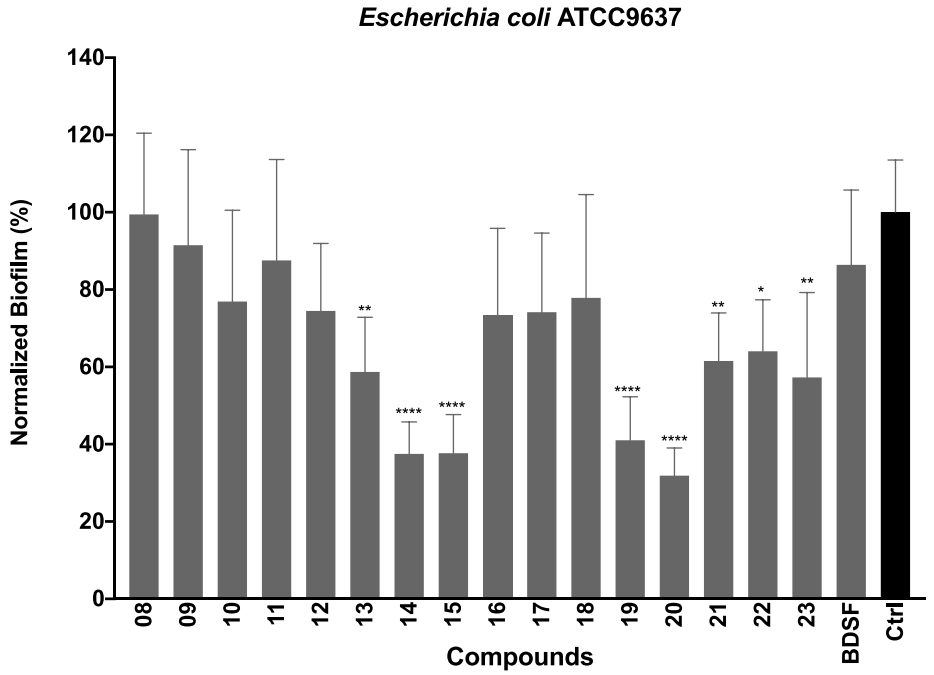


Fig. 7. Effect of sulfonamides on biofilm formation of *E. coli* ATCC9637 (*p < 0.05, **p < 0.01, ***p < 0.001, ****p < 0.0001).

biofilm growth across several bacterial species. This outcome matched similar findings with our earlier olefinic *N*-acyl sulfonamides, where a 2-bromobenzenesulfonamide was the standout compound. The superior activity of halogen-containing analogues may be in part due to increased lipophilicity (e.g. cLogP of 5.15 for **12** vs. cLogP of 6.04 for **13**) and improved permeation of these molecules through membranes or existing bacterial biofilms [57,58]. It is also interesting to note that the aromatic *N*-acyl sulfonamides broadly behaved in a similar manner to the parent signalling molecule BDSF for most of the species under investigation. In *A. baumannii* and *E. coli*, both BDSF and the sulfonamide analogues were observed to inhibit biofilm formation. By contrast, BDSF promoted biofilm growth in *B. cepacia*, *P. aeruginosa* and *S. maltophilia* which matched the effect of the sulfonamides. The main exception was in *B. cenocepacia* where biofilm production was inhibited by BDSF but the sulfonamides were inactive.

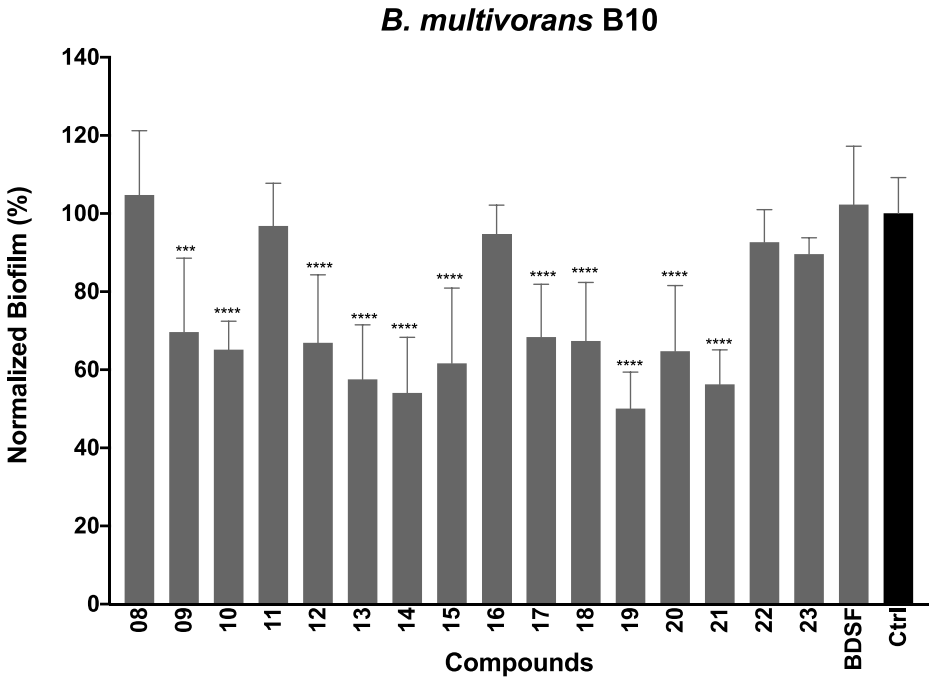


Fig. 8. Effect of sulfonamides on biofilm formation of *B. multivorans* B10 (*p < 0.05, **p < 0.01, ***p < 0.001, ****p < 0.0001).

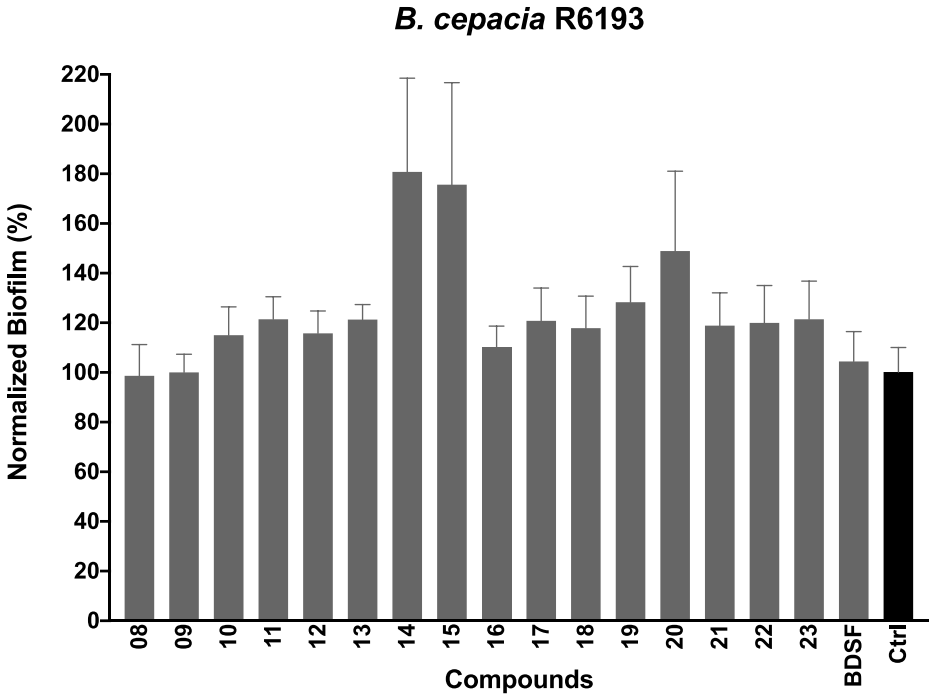


Fig. 9. Effect of sulfonamides on biofilm formation of *B. cepacia* R61993 (*p < 0.05, **p < 0.01, ***p < 0.001, ****p < 0.0001).

2.4. Colistin enhancing effects

Colistin is a last-resort antibiotic which is used to treat hospital-acquired infections caused by multi-drug resistant (MDR) Gram-negative pathogens [59]. The colistin enhancing effect of our aromatic *N*-acyl sulfonamide analogues was next investigated. Compounds were administered at a fixed dose of 50 μM concentration to the seven strains *A. baumannii* ATCC 15308, *E. coli* ATCC 9637, *B. multivorans* B10, *B. cepacia* R6193 and *B. cenocepacia* 289, *P. aeruginosa* PAO1 and *S. maltophilia* K279a. Resistance to colistin has been identified in all five genera [60–63]. The strongest colistin enhancing effects were observed in *S. maltophilia* despite these compounds not inhibiting biofilm formation in this bacterium (Fig. 5). The MIC values were at least 2-fold lower than the DMSO control (2 μg/mL) in the presence of a majority of our compounds. Seven compounds produced a 2-4-fold improvement compared to the DMSO control, namely methylsulfonamide **8** (entry 4), *tert*-butylsulfonamide **10** (entry 6), 3,3,3-trifluoropropylsulfonamide **11** (entry 7), phenylsulfonamide **12** (entry 8),

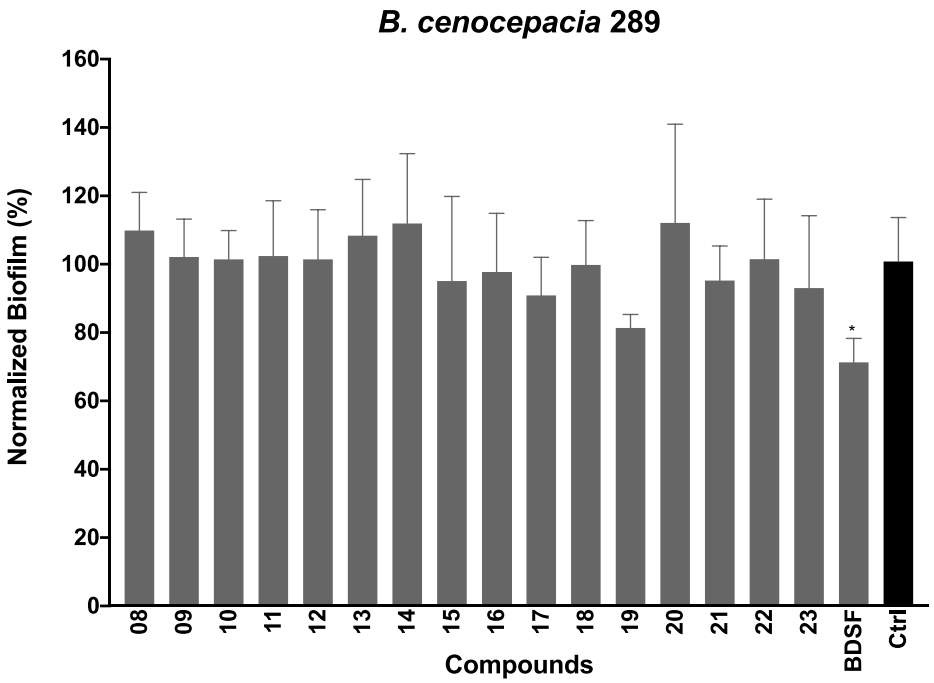


Fig. 10. Effect of sulfonamides on biofilm formation of *B. cenocepacia* 289 (*p < 0.05, **p < 0.01, ***p < 0.001, ****p < 0.0001).

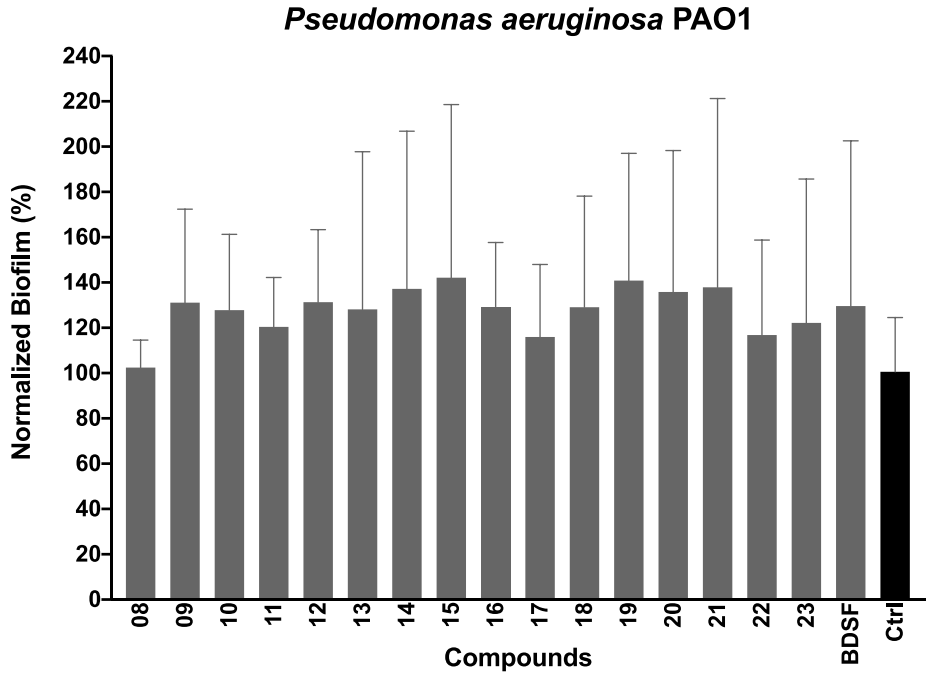


Fig. 11. Effect of sulfonamides on biofilm formation of *P. aeruginosa* PAO1 (*p < 0.05, **p < 0.01, ***p < 0.001, ****p < 0.0001).

ortho-bromophenylsulfonamide **13** (entry 9), *meta*-fluorophenylsulfonamide **17** (entry 13) and *para*-fluorophenylsulfonamide **18** (entry 14). This is well below the threshold required for use in colistin inhalation therapy [63]. Cyclopropylsulfonamide **9** (entry 5), *ortho*-fluorophenylsulfonamide **16** (entry 12), *para*-methoxyphenylsulfonamide **22** (entry 18) and *para*-nitrophenylsulfonamide **23** (entry 19) were also found to reduce the MIC to 1 μg/mL which represented a 2-fold improvement compared to colistin alone.

Although most sulfonamides inhibited biofilm formation in *A. baumannii* (Fig. 5), this did not directly translate to increased colistin sensitivity. Only two compounds exhibited an enhancing effect with a 2-fold reduction in MIC noted for methylsulfonamide **8** (entry 4) and cyclopropylsulfonamide **9** (entry 5). No reduction in MIC values was observed in *E. coli* even though biofilm production was also disrupted in this species.

Neither *B. multivorans* B10, *B. cepacia* R6493 or *B. cenocepacia* 289 responded to any colistin/analogue combination and MIC values remained unchanged. Additionally, none of our aromatic *N*-acyl sulfonamides displayed an antibiotic enhancing effect in *P. aeruginosa*.

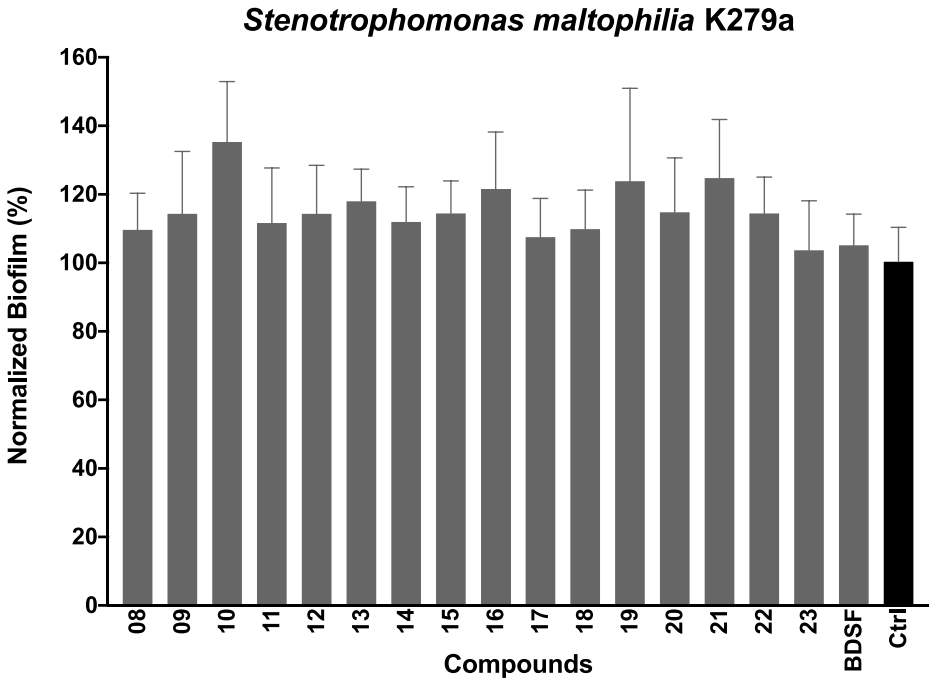


Fig. 12. Effect of sulfonamides on biofilm formation of *S. maltophilia* K279a (*p < 0.05, **p < 0.01, ***p < 0.001, ****p < 0.0001).

Surprisingly, halogenated sulfonamides **14** (entry 10), **15** (entry 11) and **20** (entry 16) increased resistance levels to colistin in all strains except *Burkholderia*. The MIC values were between 2- and 8-fold higher than the DMSO control suggesting these analogues were protecting the bacterial cells from the effects of colistin.

Galleria mellonella has been widely used as an effective model to evaluate the efficacy of antimicrobial compounds [64]. Based on the reduction in MIC observed in *S. maltophilia*, we decided to investigate the *in vivo* effects of sulfonamides **8**, **10**, **14** and **20** on *G. mellonella*. *G. mellonella* is increasingly popular both as a means of measuring chemical toxicity [65] and as a model for bacterial lung infections [66]. When the selected sulfonamides were initially screened for toxicity at 50 μM concentration, larval survival reached 100% for all compounds tested (data not shown). Given their apparent non-toxicity *in vivo*, *G. mellonella* larvae were infected with *S. maltophilia* K279a and treated with colistin alone or in combination with the sulfonamides. Of the four sulfonamides examined, *tert*-butylsulfonamide **10** was the most effective and showed an improvement in larval survival when combined with colistin compared to untreated larvae or larvae treated with colistin alone (Fig. 13). Although sulfonamide **10** was not associated with a decrease in biofilm formation in *S. maltophilia*, co-administration with colistin did result in a 2–4 fold reduction in MIC (Table 2, entry 6). These results, which mirror similar trends in the olefinic sulfonamides [15], suggest that *tert*-butylsulfonamide **10** is a good enhancer of colistin activity although the exact mechanism involved in the survival improvement remains to be elucidated.

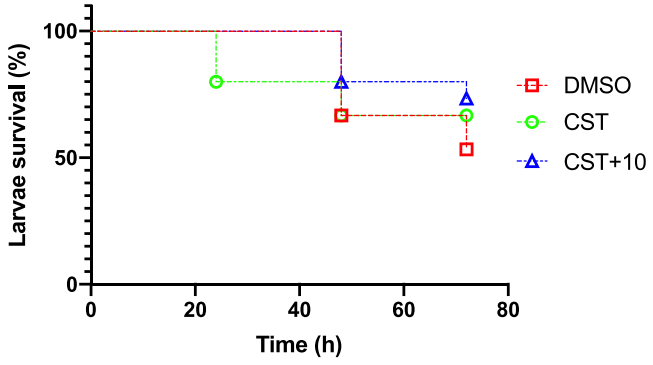


Fig. 13. Kaplan-Meier survival curves of *Galleria mellonella* infected with *S. maltophilia* K279a. *G. mellonella* was treated with colistin (CST) at MIC 0.5 μg/mL or in combination with sulfonamide **10** at 50 μM in PBS. DMSO at 0.5% in PBS was used as a vehicle control for untreated larvae.

3. Conclusion

The DSF family of compounds are all characterised by the presence of a *cis*-alkene which lies in conjugation with a carboxylic acid. Several studies have highlighted the importance of the configuration of the double bond, with the corresponding *trans*-isomers possessing little or no biological activity. We have previously demonstrated that replacing the carboxylic acid in BDSF with an *N*-acyl sulfonamide affords compounds with the ability to inhibit biofilm production and enhance colistin sensitivity in BDSF-sensitive bacteria. However, the preparation of these compounds is problematic due to tendency of the *cis*-alkene to isomerise.

In this work, we have created a second generation library of compounds where the *cis*-alkene is replaced with a benzene ring. Despite this structural modification, the resulting aromatic *N*-acyl sulfonamides retained biological activity, with several molecules significantly inhibiting biofilm production in *A. baumannii, E. coli* and *B. multivorans*. The strongest effects were observed in *E. coli* with halogenated analogues **14**, **15**, **19** and **20** proving most potent. There was a degree of overlap in *B. multivorans* with the same halogen-containing molecules among the most effective biofilm inhibitors. Additionally, in the case of *A. baumannii* and *E. coli*, the sulfonamide library did not affect cell growth, suggesting likely inhibition *via* interference with QS-regulated biofilm production. The inhibition of biofilm growth did not directly result in decreased antibiotic tolerance, however, with only a 2-fold reduction in colistin MIC recorded for *A. baumannii* and no reduction observed in *E. coli*. By contrast, several aromatic *N*-acyl sulfonamides caused a reduction in colistin MIC in *S. maltophilia*, despite not affecting biofilm growth in this species, matching our earlier findings with

Table 2
Minimal inhibitory concentrations (MIC) to colistin of *A. baumannii* ATCC 15308 (ABA), *E. coli* ATCC 9637 (ECO), *B. multivorans* B10 (BMU), *B. cepacia* R6193 (BCE), *B. cenocepacia* 289 (BCN), *P. aeruginosa* (PAO) and *S. maltophilia* K279a (SMA) isolates in the presence of sulfonamides at a fixed dose of 50 μM.

Entry	Compound	Colisin MIC (μg/ml)						
		ABA	*ECO*	*BMU*	*BCE*	*BCN*	*PAO*	SMA
1	w/o	0.25–0.5	0.125–0.25	>128	>256	>256	1–2	2–8
2	DMSO	0.25	0.0625–0.125	>128	>256	>256	1	2
3	BDSF	0.125–0.25	0.0625–0.125	>128	>256	>256	1	0.5
4	**08**	0.125–0.25	0.125	>128	>256	>256	1	0.5–1
5	**09**	0.125–0.25	0.125	>128	>256	>256	1	1
6	**10**	0.25–0.5	0.5	>128	>256	>256	1	0.5–1
7	**11**	0.25–0.5	0.25–0.5	>128	>256	>256	1	0.5–1
8	**12**	0.25–0.5	0.25–0.5	>128	>256	>256	1	0.5–1
9	**13**	0.5	0.5	>128	>256	>256	1	0.5–1
10	**14**	1	>1	>128	>256	>256	4–8	4
11	**15**	2	>1	>128	>256	>256	8	2–4
12	**16**	0.25–0.5	0.25–0.5	>128	>256	>256	1	1
13	**17**	0.25–0.5	0.25	>128	>256	>256	1	0.5–1
14	**18**	0.25–0.5	0.5	>128	>256	>256	1	0.5–1
15	**19**	1	1	>128	>256	>256	4	2
16	**20**	2	>1	>128	>256	>256	8	4
17	**21**	0.5	0.5	>128	>256	>256	1	4–8
18	**22**	0.25–0.5	0.25	>128	>256	>256	1	1
19	**23**	0.5–1	0.5	>128	>256	>256	2	1

olefinic sulfonamides. Importantly, the levels achieved are below the threshold required for colistin inhalation therapy. These *in vitro* results were reflected *in vivo* with increased *Galleria* larval survival observed on co-administration of colistin with *tert*-butylsulfonamide **10** compared to colistin alone. Taken together, these findings demonstrate the potential of aromatic *N*-acyl sulfonamide erivatives of BDSF as biofilm inhibitors and disruptors of antimicrobial resistance in pathogenic bacteria.

4. Experimental section

4.1. Chemistry

Acetonitrile, benzenesulfonamide, bis(triphenylphosphine)palladium(II) dichloride, copper ioidide, dichloromethane, diethyl ether, dimethyl formamide, hexane, lithium hydroxide, methanol, platinum (IV) oxide and triethylamine were obtained from Sigma-Aldrich. 2-Bromobenzenesulfonamide, 3-bromobenzenesulfonamide, 4-bromobenzenesulfonamide, 4-*tert*-butylbenzenesulfonamide, *tert*-butylsulfonamide, 4-chlorobenzenesulfonamide, cyclopropylsulfonamide, DMAP, DCC, 2-fluorobenzenesulfonamide, 3-fluorobenzenesulfonamide, 4-fluorobenzenesulfonamide, 4-iodobenzenesulfonamide, methanesulfonamide, 4-methoxybenzenesulfonamide, 4-nitrobenzenesulfonamide and 3,3,3-trifluoropropanesulfonamide were obtained from Fluorochem Ltd. 1-Nonyne was obtained from TCI Chemicals (Europe). Unless otherwise noted, all the purchased materials and solvents were used without further purification. Compounds were purified by silica gel (Kieselgel 60, 0.040–0.063 mm, Merck) column chromatography. ^{1}H NMR and ^{13}C NMR spectra were recorded on Bruker Avance 300 (300/75 MHz) or Bruker Avance 400 (400/100 MHz) NMR spectrometers respectively. cLogP values were calculated using SwissADME [67].

4.1.1. Synthesis of methyl 2-(non-1-yn-1-yl)benzoate (5) [24]

Bis(triphenylphosphine)palladium(II) dichloride (25 mg, 0.035 mmol, 3 mol%) and copper iodide (11 mg, 0.059 mmol, 5 mol%) were added to an oven dried microwave tube. Freshly distilled triethylamine (1.60 mL, 11.501 mmol, 10.00 eq.) and **4** (312 mg, 1.191 mmol, 1.00 eq.) in dry degassed acetonitrile (6 mL) were then added to the vial before 1-nonyne (0.230 mL, 1.428 mmol, 1.20 eq.) was added. The mixture was stirred under microwave irradiation at 100 °C (120 W) for 1 h. The reaction mixture was filtered through a pad of celite, washed with water and extracted with diethyl ether (3 × 30 mL). The combined organic layers were washed with water (20 mL) and brine (20 mL) and dried with $MgSO_4$. The solution was filtered and the solvents removed *in vacuo*. The crude mixture was purified by column chromatography on silica gel using hexane-diethyl ether (100:0–98:2) to yield **5** as a pale yellow oil (270 mg, 1.048 mmol, 88%).

^{1}H NMR (400 MHz, $CDCl_3$) δ 0.89 (t, 3H, J = 6.7 Hz, C9′), 1.24–1.39 (m, 6H, C6′-C8′), 1.47 (tt, 2H, J = 7.6 Hz, C5′), 1.63 (tt, 2H, J = 7.5 Hz, C4′), 2.47 (t, 2H, J = 7.1 Hz, C3′), 3.91 (s, 3H, C8), 7.30 (ddd, 1H, J = 7.6, 1.3 Hz, C5), 7.42 (ddd, 1H, J = 7.6, 1.3 Hz, C4), 7.51 (dd, 1H, J = 7.8, 1.2 Hz, C3), 7.88 (dd, 1H, J = 7.9, 1.2 Hz, C6).

^{13}C NMR (100 MHz, $CDCl_3$) δ 14.1 (C9′, CH_3), 19.8 (C3′, CH_2), 22.7 (C8′, CH_2), 28.7 (C4′, CH_2), 28.9 (C5′, CH_2), 29.0 (C6′, CH_2), 31.8 (C7′, CH_2), 52.1 (C8, CH_3), 79.2 (C1′), 96.1 (C2'), 124.5 (C2), 127.1 (C5, CH), 130.1 (C6, CH), 131.5 (C4, CH), 131.9 (C1), 134.2 (C3, CH), 167.0 (C7).

IR (ATR) $\bar{\upsilon}_{max}$ cm^{-1} 2928, 2856, 2232, 1734, 1485, 1432, 1447, 1292, 1249, 1129, 1083, 757, 702

4.1.2. Synthesis of methyl 2-nonylbenzoate (6)

Platinum(IV) oxide hydrate (30 mg, 0.123 mmol, 5 mol%) was added to an oven-dried round bottom flask before **5** (636 mg, 2.465 mmol, 1.00 eq.) in methanol (8 mL) was added. The flask was evacuated and back filled with hydrogen gas. The suspension was stirred for 24 h under an atmosphere of hydrogen. The reaction mixture was filtered through a pad of celite and the filtrate was concentrated under reduced pressure to yield **6** as a pale yellow oil (644 mg, 2.461 mmol, 100%).

^{1}H NMR (400 MHz, $CDCl_3$) δ 0.80 (t, 3H, J = 6.8 Hz, C9′), 1.11–1.39 (m, 12H, C3′-C8′), 1.57 (tt, 2H, J = 7.5 Hz, C2′), 2.86 (t, 2H, J = 7.8 Hz, C1′), 3.82 (s, 3H, C8), 7.12–7.24 (m, 2H, C3, C5). 7.33 (ddd, 1H, J = 7.6, 1.1 Hz, C4), 7.77 (dd, 1H, J = 8.0, 0.9 Hz, C6).

^{13}C NMR (100 MHz, $CDCl_3$) δ 14.1 (C9′, CH_3), 22.7 (C8′, CH_2), 29.4 (CH_2), 29.6 (CH_2), 29.60 (CH_2), 29.8 (C3′, CH_2), 31.8 (C2′, CH_2), 31.9 (C7′, CH_2), 34.5 (C1', CH_2), 51.9 (C8, CH_3), 125.6 (C5, CH), 129.5 (C1), 130.5 (C6, CH), 130.9 (C3, CH), 131.8 (C4, CH), 144.8 (C2), 168.3 (C7).

IR (ATR) $\bar{\upsilon}_{max}$ cm^{-1} 3483, 2924, 2854, 1725, 1433, 1253, 1102, 1078, 750, 710

HRMS (ESI) *m/z*: [M+H] Calcd for $C_{17}H_{26}O_2$ 263.2005; Found 263.2016.

4.1.3. Synthesis of 2-nonylbenzoic acid (7) [68]

Methyl 2-nonylbenzoate (**6**) (670 mg, 2.557 mmol, 1.00 eq.) and lithium hydroxide (336 mg, 14.000 mmol, 5.50 eq.) were dissolved in THF/methanol/water 3:1:1 (20 mL) and refluxed overnight in a round bottom flask. The reaction mixture was cooled to room temperature before the solvent was removed under reduced pressure. Water (15 m L) was added and the mixture was acidified to pH 2 using 2 M aqueous HCl

(15 mL) before extracting with diethyl ether (5 × 30 mL). The combined organic extracts were washed with brine, dried with $MgSO_4$, filtered, and evaporated *in vacuo* to yield **7** as a pale yellow oil (596 mg, 2.403 mmol, 94%).

^{1}H NMR (400 MHz, $CDCl_3$) δ 0.86 (t, 3H, J = 6.7 Hz, C9′), 1.16–1.46 (m, 12H, C3′-8′), 1.62 (tt, 2H, J = 7.5 Hz, C2′), 3.02 (t, 2H, J = 7.8 Hz, C1′), 7.20–7.33 (m, 2H, C3, C5), 7.46 (ddd, 1H, J = 7.41 Hz, C4), 7.97–8.09 (m, 1H, C6).

^{13}C NMR (100 MHz, $CDCl_3$) δ 14.1 (C9′, CH_3), 22.7 (C8′, CH_2), 29.4 (C6′, CH_2), 29.5 (C5′, CH_2), 29.6 (C4′, CH_2), 29.8 (C3′, CH_2), 31.8 (C2′, CH_2), 31.9 (C7′, CH_2), 34.6 (C1', CH_2), 125.8 (C5, CH), 128.1 (C1), 131.2 (C3, CH), 131.6 (C6, CH), 132.8 (C4, CH), 146.0 (C2), 173.2 (C7).

IR (ATR) $\bar{\upsilon}_{max}$ cm^{-1} 2923, 2853, 1688, 1456, 1403, 1297, 1264, 907, 733, 656, 561

HRMS (ESI) *m/z*: [M+Na] Calcd for $C_{22}H_{37}NO_3S$ 271.1668; Found 271.1672.

4.1.4. General procedure for the preparation of N-(sulfonyl)-2-nonylbenzamides

A solution of 2-nonylbenzoic acid (50 mg, 0.202 mmol, 1.00 eq.) and DMAP (27 mg, 0.221 mmol, 1.10 eq.) in DCM (5 mL) was cooled to 0 °C before the appropriate sulfonamide (0.192 mmol, 0.95 eq.) was added. After stirring for 15 min under a nitrogen atmosphere, DCC (45 mg, 0.221 mmol, 1.10 eq.) was added and the mixture was stirred for 16 h at room temperature. The reaction mixture was filtered through a thin pad of celite to remove the insoluble urea and the solvent was removed *in vacuo*. The resulting residue was redissolved in diethyl ether (10 mL), poured onto 2 M aqueous HCl (20 mL) and extracted with diethyl ether (3 × 30 mL). The combined organic extracts were washed with brine (20 mL), dried over $MgSO_4$ and filtered. The solvent was removed *in vacuo* and the resulting residue was purified by silica gel column chromatography using hexane-diethyl ether (70:30) to afford the target sulfonamide.

4.1.5. N-(Methanesulfonyl)-2-nonylbenzamide (8)

Prepared following the general procedure using 2-nonylbenzoic acid (**7**) (50 mg, 0.202 mmol, 1.00 eq.), DMAP (27 mg, 0.221 mmol, 1.10 eq.), methanesulfonamide (18 mg, 0.192 mmol, 0.95 eq.) and DCC (45 mg, 0.221 mmol, 1.10 eq.) in DCM (5 mL). The crude mixture was purified by column chromatography on silica gel using hexane-diethyl ether (70:30) to yield **8** as an off-white solid (51 mg, 0.157 mmol, 82%), mp 57–59 °C.

^{1}H NMR (400 MHz, $CDCl_3$) δ 0.87 (t, 3H, J = 6.8 Hz, C9′), 1.16–1.40 (m, 12H, C3′-C8′), 1.53–1.67 (m, 2H, C2′), 2.82 (t, 2H, J = 7.9 Hz, C1′), 3.43 (s, 3H, C8), 7.22–7.34 (m, 2H, C3, C5), 7.40–7.50 (m, 2H, C4, C6), 8.24 (s, 1H, N–H).

^{13}C NMR (100 MHz, $CDCl_3$) δ 14.1 (C9′, CH_3), 22.7 (C8′, CH_2), 29.3 (CH_2), 29.4 (CH_2), 29.5 (C4′, CH_2), 29.6 (C3′, CH_2), 31.9 (C2′, C7′, 2 × CH2), 33.4 (C1', CH_2), 41.6 (C8, CH_3), 126.1 (C5, CH), 127.2 (C6, CH), 131.2 (C3, CH), 131.8 (C1), 132.1 (C4, CH), 143.1 (C2), 167.4 (C7).

IR (ATR) $\bar{\upsilon}_{max}$ cm^{-1} 3232, 2925, 2854, 1698, 1435, 1403, 1341, 1164, 972, 893, 750, 520

HRMS (ESI) *m/z*: [M+H] Calcd for $C_{17}H_{27}NO_3S$ 326.1784; Found 326.1780.

4.1.6. N-(Cyclopropanesulfonyl)-2-nonylbenzamide (9)

Prepared following the general procedure using 2-nonylbenzoic acid (**7**) (50 mg, 0.202 mmol, 1.00 eq.), DMAP (27 mg, 0.221 mmol, 1.10 eq.), cyclopropylsulfonamide (23 mg, 0.192 mmol, 0.95 eq.) and DCC (45 mg, 0.221 mmol, 1.10 eq.) in DCM (5 mL). The crude mixture was purified by column chromatography on silica gel using hexane-diethyl ether (70:30) to yield **9** as an off-white solid (39 mg, 0.111 mmol, 58%), mp 50–52 °C.

^{1}H NMR (300 MHz, $CDCl_3$) δ 0.87 (t, 3H, J = 6.8 Hz, C9′), 1.12–1.20 (m, 2H, C2″, C3″), 1.20–1.38 (m, 12H, C3′-C8′), 1.40–1.47 (m, 2H, C2″, C3″), 1.61 (tt, 2H, J = 7.5 Hz, C2′), 2.82 (t, 2H, J = 7.8 Hz, C1′), 3.09–3.18 (m, 1H, C1″), 7.21–7.33 (m, 2H, C3, C5), 7.39–7.48 (m, 2H, C4, C6), 8.17 (s, 1H, N–H).

^{13}C NMR (75 MHz, $CDCl_3$) δ 6.3 (C2″, C3″, 2 × CH2), 14.1 (C9′, CH_3), 22.7 (C8′, CH_2), 29.3 (CH_2), 29.5 (CH_2), 29.5 (CH_2), 29.6 (CH_2), 31.3 (C1'', CH), 31.8 (C2′, CH_2), 31.9 (C7′, CH_2), 33.4 (C1', CH_2), 126.1 (C5, CH), 127.1 (C6, CH), 131.0 (C3, CH), 131.8 (C4, CH), 132.3 (C1), 142.7 (C2), 167.2 (C7).

IR (ATR) $\bar{\upsilon}_{max}$ cm^{-1} 3232, 2925, 2854, 1698, 1455, 1427, 1344, 158, 1059, 1042, 885, 847, 750, 574

HRMS (ESI) *m/z*: [M+H] Calcd for $C_{19}H_{29}NO_3S$ 352.1941; Found 352.1943.

4.1.7. N-(tert-Butylsulfonyl)-2-nonylbenzamide (10)

Prepared following the general procedure using 2-nonylbenzoic acid (**7**) (50 mg, 0.202 mmol, 1.00 eq.), DMAP (27 mg, 0.221 mmol, 1.10 eq.), *tert*-butylsulfonamide (26 mg, 0.192 mmol, 0.95 eq.) and DCC (45 mg, 0.221 mmol, 1.10 eq.) in DCM (5 mL). The crude mixture was purified by column chromatography on silica gel using hexane-diethyl ether (70:30) to yield **10** as a yellow solid (51 mg, 0.139 mmol, 73%), mp 52–53 °C.

^{1}H NMR (500 MHz, $CDCl_3$) δ 0.87 (t, 3H, J = 6.9 Hz, C9′), 1.19–1.38 (m, 12H, C3′-C8′), 1.56 (s, 9H, C2″-C4″), 1.57–1.67 (m, 2H, C2′), 2.80 (t, 2H, J = 7.9 Hz, C1′), 7.22–7.31 (m, 2H, C3, C4), 7.38–7.47 (m, 2H, C5, C6), 7.78 (s, 1H, N–H).

^{13}C NMR (125 MHz, $CDCl_3$) δ 14.1 (C9′, CH_3), 22.7 (C8′, CH_2), 24.5 (C2″-C4″, 3 × CH_3), 29.3 (CH_2), 29.5 (CH_2), 29.5 (CH_2), 29.6 (CH_2), 31.9 (C7′, CH_2), 32.0 (C2′, CH_2), 33.4 (C1′, CH_2), 62.5 (C1″), 126.0 (C5, CH), 127.0 (C6, CH), 130.8 (C3, CH), 131.5 (C4, CH), 133.2 (C1), 142.4 (C2), 166.8 (C7).

IR (ATR) $\bar{\upsilon}_{max}$ cm^{-1} 3236, 2925, 2854, 1714, 1448, 1429, 1332, 1259, 1139, 1056, 843, 801, 649, 567, 511

HRMS (ESI) *m/z*: [M+H] Calcd for $C_{20}H_{33}NO_3S$ 368.2254; Found 368.2251.

4.1.8. 2-Nonyl-N-(3,3,3-trifluoropropanesulfonyl)benzamide (11)

Prepared following the general procedure using 2-nonylbenzoic acid (**7**) (50 mg, 0.202 mmol, 1.00 eq.), DMAP (27 mg, 0.221 mmol, 1.10 eq.), 3,3,3-trifluoropropanesulfonamide (34 mg, 0.192 mmol, 0.95 eq.) and DCC (45 mg, 0.221 mmol, 1.10 eq.) in DCM (5 mL). The crude mixture was purified by column chromatography on silica gel using hexane-diethyl ether (90:10) to yield **11** as a yellow waxy solid (27 mg, 0.066 mmol, 36%).

^{1}H NMR (400 MHz, $CDCl_3$) δ 0.87 (t,3H, J = 6.9 Hz, C9′), 1.21–1.38 (m,12H, C3′-C8′), 1.54–1.64 (m, 2H, C2′), 2.66–2.78 (m,2H, C2″), 2.81 (t, 2H, J = 7.9 Hz, C1′), 3.77–3.85 (m, 2H, C1″), 7.24–7.34 (m,2H, C3, C5), 7.43–7.50 (m, 2H, C4, C6).

^{13}C NMR (100 MHz, $CDCl_3$) δ 14.1 (C9′, CH_3), 22.7 (C8′, CH_2), 28.8 (d, $^2J_{C\text{-}F}$ = 31.6, C2″, CH_2), 29.3 (CH_2), 29.4 (CH_2), 29.5 (CH_2), 29.6 (CH_2), 31.9 (C14, CH_2), 32.0 (C9, CH_2), 33.4 (C1', CH_2), 46.9 (d, $^3J_{C\text{-}F}$ = 3.3 Hz, C1'', CH_2), 125.2 (d, $^1J_{C\text{-}F}$ = 276.8 Hz, CF_3), 126.2 (C3, CH), 127.3 (C4, CH), 131.2 (C1), 131.3 (C5, CH), 132.4 (C6, CH), 143.5 (C2), 167.3 (C7).

^{19}F NMR (376 MHz, $CDCl_3$) δ −65.8 (s, CF_3).

IR (ATR) $\bar{\upsilon}_{max}$ cm^{-1} 2961, 2917, 2849, 1746, 1630, 1462, 1260, 1089, 1017, 797, 415

HRMS (ESI) *m/z*: [M+H] Calcd for $C_{19}H_{28}F_3NO_3S$ 408.1814; Found 408.1813.

4.1.9. N-(Benzenesulfonyl)-2-nonylbenzamide (12)

Prepared following the general procedure using 2-nonylbenzoic acid (**7**) (50 mg, 0.202 mmol, 1.00 eq.), DMAP (27 mg, 0.221 mmol, 1.10 eq.), benzenesulfonamide (30 mg, 0.192 mmol, 0.95 eq.) and DCC (45 mg, 0.221 mmol, 1.10 eq.) in DCM (5 mL). The crude mixture was purified by column chromatography on silica gel using hexane-diethyl ether (80:20) to yield **12** as a yellow solid (45 mg, 0.116 mmol, 61%), mp 42–43 °C.

^{1}H NMR (400 MHz, $CDCl_3$) δ 0.88 (t, 3H, $J = 6.9$ Hz, C9′), 1.04–1.39 (m, 14H, C2′-C8′), 2.59 (t, 2H, $J = 7.8$ Hz, C1′), 7.15–7.24 (m, 2H, C3, C4), 7.33–7.42 (m, 2H, C5, C6), 7.57 (dd, 2H, $J = 7.5$ Hz, C3″, C5″), 7.67 (dd, 1H, $J = 7.5$ Hz, C4″), 8.14 (d, 2H, $J = 7.5$ Hz, C2″, C6″), 8.51 (s, 1H, N–H).

^{13}C NMR (100 MHz, $CDCl_3$) δ 14.2 (C9′, CH_3), 22.7 (C8′, CH_2), 29.3 (CH_2), 29.4 (CH_2), 29.5 (CH_2), 29.6 (CH_2), 31.7 (C2′, CH_2), 31.9 (C7′, CH_2), 33.1 (C1', CH_2), 126.0 (C5, CH), 127.1 (C6, CH), 128.5 (C2″, C6″, 2 × CH), 129.0 (C3″, C5″, 2 × CH), 130.9 (C3, CH), 131.7 (C4, CH), 132.2 (C1), 134.1 (C4″, CH), 138.4 (C1''), 142.6 (C2), 166.4 (C7).

IR (ATR) $\bar{\nu}_{max}$ cm^{-1} 3238, 2925, 2854, 1705, 1450, 1428, 1349, 1172, 1089, 1059, 751, 686, 584, 566

HRMS (ESI) *m/z*: [M+H] Calcd for $C_{22}H_{29}NO_3S$ 388.1941; Found 388.1947.

4.1.10. N-(2-Bromobenzenesulfonyl)-2-nonylbenzamide (13)

Prepared following the general procedure using 2-nonylbenzoic acid (**7**) (50 mg, 0.202 mmol, 1.00 eq.), DMAP (27 mg, 0.221 mmol, 1.10 eq.), 2-bromobenzenesulfonamide (45 mg, 0.192 mmol, 0.95 eq.) and DCC (45 mg, 0.221 mmol, 1.10 eq.) in DCM (5 mL). The crude mixture was purified by column chromatography on silica gel using hexane-diethyl ether (85:15) to yield **13** as an off-white solid (59 mg, 0.126 mmol, 67%), mp 116–118 °C.

^{1}H NMR (400 MHz, $CDCl_3$) δ 0.81 (t, 3H, $J = 6.8$ Hz, C9′), 1.03–1.28 (m, 12H, C3′-8′), 1.28–1.42 (m, 2H, C2′), 2.59 (t, 2H, $J = 7.8$ Hz, C1′), 7.21–7.29 (m, 2H, C3, C5), 7.41 (dt, 1H, $J = 7.6$, 1.3 Hz, C4), 7.46–7.54 (m, 2H, C6, C4″), 7.58 (ddd, 1H, $J = 7.7$, 1.2 Hz, C5″), 7.75 (dd, 1H, $J = 7.7$, 1.2 Hz, C3″), 8.42 (dd, 1H, $J = 7.9$, 1.8 Hz, C6″), 8.67 (s, 1H, N–H).

^{13}C NMR (100 MHz, $CDCl_3$) δ 14.2 (C9′, CH_3), 22.8 (C8′, CH_2), 29.3 (2 × CH_2), 29.5 (CH_2), 29.6 (CH_2), 31.7 (C2′, CH_2), 31.9 (C7′, CH_2), 33.1 (C1', CH_2), 120.0 (C2″), 126.0 (C5, CH), 127.2 (C6, CH), 128.0 (C5″, CH), 131.0 (C3, CH), 131.8 (C1), 131.9 (C4, CH), 133.8 (C6″, CH), 134.9 (C4″, CH), 135.1 (C3″, CH), 137.6 (C1''), 143.1 (C2), 166.1 (C7).

IR (ATR) $\bar{\nu}_{max}$ cm^{-1} 3247, 2923, 2852, 1707, 1575, 1416, 1345, 1177, 1051, 1024, 581

HRMS (ESI) *m/z*: Calcd for $C_{22}H_{28}BrNO_3S$ 466.1046; Found 466.1044.

4.1.11. N-(3-Bromobenzenesulfonyl)-2-nonylbenzamide (14)

Prepared following the general procedure using 2-nonylbenzoic acid (**7**) (50 mg, 0.202 mmol, 1.00 eq.), DMAP (27 mg, 0.221 mmol, 1.10 eq.), 3-bromobenzenesulfonamide (45 mg, 0.192 mmol, 0.95 eq.) and DCC (45 mg, 0.221 mmol, 1.10 eq.) in DCM (5 mL). The crude mixture was purified by column chromatography on silica gel using hexane-diethyl ether (85:15) to yield **14** as an off-white solid (76 mg, 0.163 mmol, 86%), mp 68–70 °C.

^{1}H NMR (300 MHz, $CDCl_3$) δ 0.88 (t, 3H, $J = 6.8$ Hz, C9′), 1.09–1.42 (m, 14H, C2′-C8′), 2.62 (t, 2H, $J = 7.8$ Hz, C1′), 7.18–7.27 (m, 2H, C3, C5), 7.34–7.42 (m, 2H, C4, C6), 7.45 (dd, 1H, $J = 8.0$ Hz, C5″), 7.79 (ddd, 1H, $J = 8.0$, 1.8, 1.0 Hz, C4″), 8.11 (ddd, 1H, $J = 8.0$, 1.8, 1.0 Hz, C6″), 8.26 (dd, 1H, $J = 1.8$ Hz, C2″), 8.35 (s, 1H, N–H).

^{13}C NMR (75 MHz, $CDCl_3$) δ 14.1 (C9′, CH_3), 22.7 (C8′, CH_2), 29.3 (CH_2), 29.4 (CH_2), 29.5 (CH_2), 29.6 (CH_2), 31.7 (C2′, CH_2), 31.9 (C7′, CH_2), 33.2 (C1', CH_2), 122.8 (C3″), 126.1 (C5, CH), 127.0 (C6, CH), 127.3 (C6″, CH), 130.4 (C5″, CH), 131.0 (C3, CH), 131.2 (C2″, CH), 131.8 (C4, CH), 131.9 (C1), 137.1 (C4″, CH), 140.3 (C1''), 142.8 (C2), 166.2 (C7).

IR (ATR) $\bar{\nu}_{max}$ cm^{-1} 3233, 2924, 2853, 1693, 1428, 1350, 1173, 1066, 892, 784, 677, 588

HRMS (ESI) *m/z*: Calcd for $C_{22}H_{28}BrNO_3S$ 466.1046; Found 466.1043.

4.1.12. N-(4-Bromobenzene)sulfonyl)-2-nonylbenzamide (15)

Prepared following the general procedure using 2-nonylbenzoic acid (**7**) (50 mg, 0.400 mmol, 1.00 eq.), DMAP (27 mg, 0.221 mmol, 1.10 eq.), 4-bromobenzenesulfonamide (45 mg, 0.192 mmol, 0.95 eq.) and DCC (45 mg, 0.221 mmol, 1.10 eq.) in DCM (5 mL). The crude mixture was purified by column chromatography on silica gel using hexane-diethyl ether (85:15) to yield **15** as an off-white solid (64 mg, 0.144 mmol, 72%), mp 94–96 °C.

^{1}H NMR (300 MHz, $CDCl_3$) δ 0.88 (t, 3H, $J = 6.8$ Hz, C9′), 1.07–1.41 (m, 14H, C2′-C8′), 2.61 (t, 2H, $J = 7.8$ Hz, C1′), 7.16–7.27 (m, 2H, C3, C5), 7.32–7.42 (m, 2H, C4, C6), 7.70 (app. dt, 2H, $J = 8.7$, 2.2 Hz, C3″, C5″), 8.00 (app. dt, 2H, $J = 8.7$, 2.2 Hz, C2″, C6″), 8.37 (s, 1H, N–H).

^{13}C NMR (75 MHz, $CDCl_3$) δ 14.1 (C9′, CH_3), 22.7 (C8′, CH_2), 29.3 (CH_2), 29.4 (CH_2), 29.5 (CH_2), 29.6 (C3′, CH_2), 31.7 (C2′, CH_2), 31.9 (C7′, CH_2), 33.2 (C1', CH_2), 126.0 (C5, CH), 127.1 (C6, CH), 129.4 (C4″), 130.1 (C2″, C6″, 2 × CH), 130.9 (C3, CH), 131.8 (C4, CH), 132.0 (C1), 132.3 (C3″, C5″, 2 × CH), 137.4 (C1''), 142.7 (C2), 166.3 (C7).

IR (ATR) $\bar{\nu}_{max}$ cm^{-1} 3234, 2923, 2853, 1686, 1574, 1428, 1351, 1172, 1068, 738, 602, 567

HRMS (ESI) *m/z*: Calcd for $C_{22}H_{28}BrNO_3S$ 466.1046; Found 466.1042.

4.1.13. Synthesis of N-(2-Fluorobenzenesulfonyl)-2-nonylbenzamide (16)

Prepared following the general procedure using 2-nonylbenzoic acid (**7**) (50 mg, 0.202 mmol, 1.00 eq.), DMAP (27 mg, 0.221 mmol, 1.10 eq.), 2-fluorobenzenesulfonamide (33 mg, 0.192 mmol, 0.95 eq.) and DCC (45 mg, 0.221 mmol, 1.10 eq.) in DCM (5 mL). The crude mixture was purified by column chromatography on silica gel using hexane-diethyl ether (85:15) to yield **16** as a white solid (51 mg, 0.126 mmol, 66%), mp 53–54 °C.

^{1}H NMR (400 MHz, $CDCl_3$) δ 0.88 (t, 3H, $J = 6.9$ Hz, C9′), 1.10–1.35 (m, 12H, C3′-8′). 1.35–1.48 (m, 2H, C2′), 2.65 (t, 2H, $J = 7.8$ Hz, C1′), 7.18–7.30 (m, 3H, C3, C5, C3″), 7.33–7.48 (m, 3H, C4, C6, C5″), 7.62–7.73 (m, 1H, C4″), 8.18 (ddd, 1H, $J = 7.6$, 1.4 Hz, C6″), 8.64 (s, 1H, N–H).

^{13}C NMR (100 MHz, $CDCl_3$) δ 14.2 (C9′, CH_3), 22.7 (C8′, CH_2), 29.3 (CH_2), 29.4 (CH_2), 29.5 (CH_2), 29.6 (CH_2), 31.6 (C2′, CH_2), 31.9 (C7′, CH_2), 33.1 (C1', CH_2), 116.9 (d, $^2J_{C\text{-}F} = 20.7$ Hz, C3″, CH), 124.7 (d, $^4J_{C\text{-}F} = 3.8$ Hz, C5″, CH), 126.1 (C5, CH), 126.5 (d, $^2J_{C\text{-}F} = 12.5$ Hz, C1″), 127.2 (C6, CH), 131.0 (C3, CH), 131.8 (C1, CH), 131.9 (C4, CH), 132.4 (C6″, CH), 136.4 (d, $^3J_{C\text{-}F} = 8.8$ Hz, C4″, CH), 143.0 (C2), 159.0 (d, $^1J_{C\text{-}F} = 256.5$ Hz, C2'', C–F), 166.3 (C7).

^{19}F NMR (376 MHz, $CDCl_3$) δ −109.8 (s, C–F).

IR (ATR) $\bar{\nu}_{max}$ cm^{-1} 3247, 2925, 2854, 1708, 1599, 1477, 1413, 1352, 1176, 1054, 761, 587

HRMS (ESI) *m/z*: [M+H] Calcd for $C_{22}H_{28}NO_3SF$ 406.1846; Found 406.1849.

4.1.14. N-(3-Fluorobenzenesulfonyl)-2-nonylbenzamide (17)

Prepared following the general procedure using 2-nonylbenzoic acid (**7**) (50 mg, 0.202 mmol, 1.00 eq.), DMAP (27 mg, 0.221 mmol, 1.10 eq.), 3-fluorobenzenesulfonamide (33 mg, 0.192 mmol, 0.95 eq.) and DCC (45 mg, 0.221 mmol, 1.10 eq.) in DCM (5 mL). The crude mixture was purified by column chromatography on silica gel using hexane-diethyl ether (85:15) to yield **17** as a white solid (56 mg, 0.138 mmol, 73%), mp 75–77 °C.

^{1}H NMR (300 MHz, $CDCl_3$) δ 0.88 (t, 3H, $J = 6.8$ Hz, C9′), 1.09–1.43 (m, 14H, C2′-C8′), 2.62 (t, 2H, $J = 7.8$ Hz, C1′), 7.16–7.28 (m, 2H, C3, C5), 73.1–7.45 (m, 3H, C4, C6, C4″), 7.56 (app dt., 1H, $J = 8.1$, 5.2 Hz, C5″), 7.85 (app. dt, 1H, $J = 8.0$, 2.1 Hz, C2″), 7.91–8.01 (m, 1H, C6″), 8.34 (s, 1H, N–H).

^{13}C NMR (75 MHz, $CDCl_3$) δ 14.1 (C9′, CH_3), 22.7 (C8′, CH_2), 29.3 (CH_2), 29.4 (CH_2), 29.5 (CH_2), 29.5 (CH_2), 31.7 (C2′, CH_2), 31.9 (C7′, CH_2), 33.2 (C1', CH_2), 115.9 (d, $^2J_{C\text{-}F} = 25.0$ Hz, C2″, CH), 121.3 (d, $^2J_{C\text{-}F} = 21.3$ Hz, C4″, CH), 124.4 (d, $^4J_{C\text{-}F} = 3.5$ Hz, C6″, CH), 126.1 (C5, CH), 127.0 (C6, CH), 130.7 (d, $^3J_{C\text{-}F} = 7.7$ Hz, C5″, CH), 131.0 (C3, CH), 131.8 (C4, CH), 132.0 (C1), 140.4 (d, $^3J_{C\text{-}F} = 7.2$ Hz, C1″), 142.8 (C2), 162.2 (d, $^1J_{C\text{-}F} = 252.1$ Hz, C3''), 166.2 (C7).

^{19}F NMR (282 MHz, $CDCl_3$) δ −109.3 (s, C–F).

IR (ATR) $\bar{\upsilon}_{max}$ cm^{-1} 3243, 2925, 2854, 1693, 1598, 1436, 1350, 1228, 1168, 1059, 902, 677, 599, 580

HRMS (ESI) *m/z*: [M+H] Calcd for $C_{22}H_{28}NO_3SF$ 406.1846; Found 406.1846.

4.1.15. N-(4-Fluorobenzenesulfonyl)-2-nonylbenzamide (18)

Prepared following the general procedure using 2-nonylbenzoic acid (**7**) (50 mg, 0.202 mmol, 1.00 eq.), DMAP (27 mg, 0.221 mmol, 1.10 eq.), 4-fluorobenzenesulfonamide (33 mg, 0.192 mmol, 0.95 eq.) and DCC (45 mg, 0.221 mmol, 1.10 eq.) in DCM (5 mL). The crude mixture was purified by column chromatography on silica gel using hexane-diethyl ether (85:15) to yield **18** as a white solid (44 mg, 0.108 mmol, 57%), mp 112–115 °C.

^{1}H NMR (300 MHz, $CDCl_3$) δ 0.88 (t, 3H, $J = 6.7$ Hz, C9′), 1.08–1.41 (m, 14H, C2′-C8′), 2.61 (t, 2H, $J = 7.8$ Hz, C1′), 7.15–7.30 (m, 4H, C3, C5, C3″, C5″), 7.32–7.43 (m, 2H, C4, C6), 8.10–8.22 (m, 2H, C2″, C6″), 8.50 (s, 1H, N–H).

^{13}C NMR (75 MHz, $CDCl_3$) δ 14.1 (C9′, CH_3), 22.7 (C8′, CH_2), 29.3 (CH_2), 29.4 (CH_2), 29.5 (2 × CH2), 31.7 (C2′, CH_2), 31.9 (C7′, CH_2), 33.2 (C1', CH_2), 116.2 (d, $^2J_{C\text{-}F} = 22.8$ Hz, C3″, C5″), 126.0 (C5, CH), 127.1 (C6, CH), 130.9 (C3, CH), 131.6 (d, $^3J_{C\text{-}F} = 9.9$ Hz, C2″, C6″), 131.7 (C4, CH), 132.1 (C1), 134.4 (d, $^4J_{C\text{-}F} = 3.1$ Hz, C1″), 142.7 (C2), 166.0 (d, $^1J_{C\text{-}F} = 256.8$ Hz, C4"), 166.4 (C7).

^{19}F NMR (282 MHz, $CDCl_3$) δ −102.6 (s, C–F).

IR (ATR) $\bar{\upsilon}_{max}$ cm^{-1} 3234, 2925, 2854, 1682, 1591, 1493, 1432, 1352, 1235, 1176, 1156, 838, 570, 546

HRMS (ESI) *m/z*: [M+H] Calcd for $C_{22}H_{28}NO_3SF$ 406.1846; Found 406.1852.

4.1.16. N-(4-Chlorobenzenesulfonyl)-2-nonylbenzamide (19)

Prepared following the general procedure using 2-nonylbenzoic acid (**7**) (50 mg, 0.202 mmol, 1.00 eq.), DMAP (27 mg, 0.221 mmol, 1.10 eq.), 4-chlorobenzenesulfonamide (36 mg, 0.192 mmol, 0.95 eq.) and DCC (45 mg, 0.221 mmol, 1.10 eq.) in DCM (5 mL). The crude mixture was purified by column chromatography on silica gel using hexane-diethyl ether (80:20) to yield **19** as a white solid (52 mg, 0.123 mmol, 64%), mp 99–101 °C.

^{1}H NMR (400 MHz, $CDCl_3$) δ 0.89 (t, 3H, $J = 7.0$ Hz, C9′), 1.09–1.41 (m, 14H, C2′-C8′), 2.62 (t, 2H, $J = 7.8$ Hz, C1′), 7.17–7.32 (m, 2H, C3, C5), 7.33–7.47 (m, 2H, C4, C6), 7.49–7.64 (m, 2H, C3″, C5″), 8.04–8.17 (m, 2H, C2″, C6″), 8.27 (s, 1H, N–H).

^{13}C NMR (100 MHz, $CDCl_3$) δ 14.2 (C9′, CH_3), 22.7 (C8′, CH_2), 29.3 (CH_2), 29.4 (CH_2), 29.5 (CH_2), 29.6 (CH_2), 31.7 (C2′, CH_2), 31.9 (C7′, CH_2), 33.2 (C1', CH_2), 126.1 (C5, CH), 127.0 (C6, CH), 129.3 (C3″, C5″, 2 × CH), 130.1 (C2″, C6″, 2 × CH), 131.0 (C3, CH), 131.9 (C4, CH), 132.0 (C1), 136.8 (C1″), 140.9 (C4"), 142.7 (C2), 166.2 (C7).

IR (ATR) $\bar{\upsilon}_{max}$ cm^{-1} 3235, 2923, 2853, 1687, 1427, 1348, 1169, 1085, 827, 753, 615, 568, 483

HRMS (ESI) *m/z*: [M+H] Calcd for $C_{22}H_{28}ClNO_3S$ 422.1551; Found 422.1541.

4.1.17. N-(4-Iodobenzenesulfonyl)-2-nonylbenzamide (20)

Prepared following the general procedure using 2-nonylbenzoic acid (**7**) (50 mg, 0.202 mmol, 1.00 eq.), DMAP (27 mg, 0.221 mmol, 1.10 eq.), 4-iodobenzenesulfonamide (54 mg, 0.192 mmol, 0.95 eq.) and DCC (45 mg, 0.221 mmol, 1.10 eq.) in DCM (5 mL). The crude mixture was purified by column chromatography on silica gel using hexane-diethyl ether (70:30) to yield **20** as an off-white solid (94 mg, 0.183 mmol, 96%), mp 66–68 °C.

^{1}H NMR (300 MHz, $CDCl_3$) δ 0.89 (t, 3H, $J = 6.8$ Hz, C9′), 1.08–1.42 (m, 14H, C2′-C8′), 2.62 (t, 2H, $J = 7.8$ Hz, C1′), 7.18–7.27 (m, 2H, C3, C5), 7.32–7.43 (m, 2H, C4, C6), 7.85 (app. dt, 2H, $J = 8.7$, 2.0 Hz, C2″, C6″), 7.94 (app. dt, 2H, $J = 8.7$, 2.0 Hz, C3″, C5″), 8.27 (s, 1H, N–H).

^{13}C NMR (75 MHz, $CDCl_3$) δ 14.1 (C9′, CH_3), 22.7 (C8′, CH_2), 29.3 (CH_2), 29.4 (CH_2), 29.5 (CH_2), 29.6 (C3′, CH_2), 31.7 (C2′, CH_2), 31.9 (C7′, CH_2), 33.2 (C1', CH_2), 102.1 (C4″), 126.1 (C5, CH), 127.0 (C6, CH), 129.9 (C2″, C6″, 2 × CH), 131.0 (C3, CH), 131.8 (C4, CH), 132.0 (C1), 138.1 (C1″), 138.3 (C3″, C5", 2 × CH), 142.7 (C2), 166.2 (C7).

IR (ATR) $\bar{\upsilon}_{max}$ cm^{-1} 3232, 2924, 2853, 1688, 1569, 1429, 1350, 1172, 1054, 1007, 730, 598, 567

HRMS (ESI) *m/z*: [M+H] Calcd for $C_{22}H_{28}INO_3S$ 514.0907; Found 514.0914.

4.1.18. N-(4-tert-Butylbenzenesulfonyl)-2-nonylbenzamide (21)

Prepared following the general procedure using 2-nonylbenzoic acid (**7**) (50 mg, 0.202 mmol, 1.00 eq.), DMAP (27 mg, 0.221 mmol, 1.10 eq.), 4-*tert*-butylbenzenesulfonamide (42 mg, 0.192 mmol, 0.95 eq.) and DCC (45 mg, 0.221 mmol, 1.10 eq.) in DCM (5 mL). The crude mixture was purified by column chromatography on silica gel using hexane-diethyl ether (70:30) to yield **21** as an off-white solid (58 mg, 0.131 mmol, 69%), mp 108–109 °C.

^{1}H NMR (300 MHz, $CDCl_3$) δ 0.88 (t, 3H, $J = 6.8$ Hz, C9′), 1.09–1.45 (m, 14H, overlapped, C2′-C8′), 1.35 (s, 9H, C9–C11), 2.62 (t, 2H, $J = 7.7$ Hz, C1′), 7.15–7.28 (m, 2H, C3, C5), 7.31–7.43 (m, 2H, C4, C6), 7.57 (app. dt, 2H, $J = 8.7$, 2.1 Hz, C3″, C5″), 8.06 (app. dt, 2H, $J = 8.7$, 2.1 Hz, C2″, C6″), 8.18 (s, 1H, N–H).

^{13}C NMR (75 MHz, $CDCl_3$) δ 14.1 (C9′, CH_3), 22.7 (C8′, CH_2), 29.3 (CH_2), 29.4 (CH_2), 29.4 (CH_2), 29.5 (CH_2), 31.0 (C9–C11, 3 × CH_3), 31.5 (C2′, CH_2), 31.9 (C7′, CH_2), 33.1 (C1', CH_2), 35.3 (C8), 126.0 (C5, C3″, C5″, 3 × CH), 126.9 (C6, CH), 128.4 (C2″, C6″, 2 × CH), 130.8 (C3, CH), 131.5 (C4, CH), 132.5 (C1), 135.4 (C1″), 142.4 (C2), 158.1 (C4"), 166.3 (C7).

IR (ATR) $\bar{\upsilon}_{max}$ cm^{-1} 3237, 2958, 2926, 2854, 1704, 1428, 1348, 1172, 1112, 846, 624, 579

HRMS (ESI) *m/z*: [M+H] Calcd for $C_{26}H_{37}NO_3S$ 444.2566; Found 444.2569.

4.1.19. N-(4-Methoxybenzenesulfonyl)-2-nonylbenzamide (22)

Prepared following the general procedure using 2-nonylbenzoic acid (**7**) (50 mg, 0.202 mmol, 1.00 eq.), DMAP (27 mg, 0.221 mmol, 1.10 eq.), 4-methoxybenzenesulfonamide (35 mg, 0.192 mmol, 0.95 eq.) and DCC (45 mg, 0.221 mmol, 1.10 eq.) in DCM (5 mL). The crude mixture was purified by column chromatography on silica gel using hexane-diethyl ether (60:40) to yield **22** as a white solid (45 mg, 0.108 mmol, 57%), mp 90–92 °C.

^{1}H NMR (300 MHz, $CDCl_3$) δ 0.88 (t, 3H, $J = 6.8$ Hz, C9′), 1.06–1.45 (m, 14H, C2′-C8′), 2.61 (t, 2H, $J = 7.8$ Hz, C1′), 3.88 (s, 3H, C8), 7.01 (app. dt, 2H, $J = 9.0$, 2.5 Hz, C3″, C5″), 7.11–7.29 (m, 2H, C3, C5), 7.29–7.43 (m, 2H, C4, C6), 8.07 (app. dt, 2H, $J = 9.0$, 2.5 Hz, C2″, C6″), 8.23 (s, 1H, N–H).

^{13}C NMR (75 MHz, $CDCl_3$) δ 14.1 (C9′, CH_3), 22.7 (C8′, CH_2), 29.3 (CH_2), 29.4 (CH_2), 29.5 (CH_2), 29.6 (CH_2), 31.6 (C2′, CH_2), 31.9 (C7′, CH_2), 33.1 (C1', CH_2), 55.7 (C8, CH_3), 114.1 (C3″, C5″, 2 × CH), 126.0 (C5, CH), 127.0 (C6, CH), 129.9 (C1″), 130.8 (C3, CH), 130.9 (C2″, C6″, 2 × CH), 131.5 (C4, CH), 132.5 (C1), 142.4 (C2), 164.0 (C4"), 166.3 (C7).

IR (ATR) $\bar{\upsilon}_{max}$ cm^{-1} 3239, 2925, 2854, 1702, 1596, 1498, 1428, 1345, 1262, 1162, 834, 574, 557

HRMS (ESI) *m/z*: [M+H] Calcd for $C_{23}H_{31}NO_4S$ 418.2046; Found 418.2054.

4.1.20. N-(4-Nitrobenzenesulfonyl)-2-nonylbenzamide (23)

Prepared following the general procedure using 2-nonylbenzoic acid (**7**) (50 mg, 0.202 mmol, 1.00 eq.), DMAP (27 mg, 0.221 mmol, 1.10 eq.), 4-nitrobenzenesulfonamide (38 mg, 0.192 mmol, 0.95 eq.) and DCC (45 mg, 0.221 mmol, 1.10 eq.) in DCM (5 mL) and DMF (1 mL). The crude mixture was purified by column chromatography on silica gel using hexane-diethyl ether (60:40) to yield **23** as an off-white solid (25 mg, 0.058 mmol, 31%), mp 120–122 °C.

^{1}H NMR (300 MHz, $CDCl_3$) δ 0.88 (t, 3H, $J = 6.9$ Hz, C9′), 1.08–1.45 (m, 14H, C2′-C8′), 2.63 (t, 2H, $J = 7.7$ Hz, C1′), 7.19–7.29 (m, 2H, C3, C5), 7.34–7.48 (m, 2H, C4, C6), 8.33–8.46 (m, 4H, C2″, C3″, C5″, C6″)

^{13}C NMR (75 MHz, $CDCl_3$) δ 14.1 (C9′, CH_3), 22.7 (C8′, CH_2), 29.3 (CH_2), 29.4 (CH_2), 29.5 (CH_2), 29.5 (CH_2), 31.8 (C2′, CH_2), 31.9 (C7′, CH_2), 33.2 (C1', CH_2), 124.1 (C3″, C5″, 2 × CH), 126.2 (C5, CH), 127.1 (C6, CH), 130.1 (C2″, C6″, 2 × CH), 131.2 (C3, CH), 131.5 (C1), 132.2 (C4, CH), 143.0 (C2), 144.0 (C1″), 151.0 (C4"), 166.1 (C7).

IR (ATR) $\bar{\upsilon}_{max}$ cm^{-1} 3110, 2926, 2853, 1678, 1529, 1432, 1350, 1185, 1174, 845, 606

HRMS (ESI) *m/z*: [M+H] Calcd for $C_{22}H_{28}N_2O_5S$ 433.1791; Found 433.1787.

4.2. Biological evaluation

4.2.1. Bacterial strains

A. baumannii ATCC 15308, *E. coli* ATCC 9637, *B. multivorans* B10, *B. cepacia* R6193, *B. cenocepacia* 289, *P. aeruginosa* PAO1 and *S. maltophilia* K279a, were the strains used in this study. Bacterial strains were obtained from our own collection. All the strains were grown in LB medium at 37 °C.

4.2.2. Intrinsic cell growth inhibition

To evaluate the growth inhibition of sulfonamides, the broth microdilution method was used, as previously described [69,70]. Briefly, bacterial strains were grown overnight in cation-adjusted Muller-Hinton Broth (cMHB) and then subcultured to new cultures with 1:100 dilution. 100 μL of fresh log phase cultures, adjusted to a final concentration of 1 × 10^5 cfu/mL, were added per well to 96-well sterile microtiter plates containing 100 μL of sulfonamides at 0.1 mM (from a stock solution at 10 mM dissolved in DMSO) to obtain a final concentration of 0.05 mM. Plates were incubated at 37 °C for 20 h and then the optical density, determined at 550 nm (OD_{550nm}), was measured using a multilabel microtitre plate reader (Victor 3, PerkinElmer LAS, Waltham, MA, USA). Before readout, plates were shaken for homogenization. DMSO alone was included as control at final concentration of 0,5%. Bacterial growth was expressed in percentage on the basis of growth in control wells. The screening was done at least two times. The average of OD_{550nm} values of each sample was used to calculate the percentage of inhibition.

4.2.3. Biofilm inhibition assay

For biofilm formation, the crystal violet method was used as previously described [71]. Briefly, 100 μl of fresh log phase bacteria at a final concentration of 1 × 10^5 cfu/mL, were added to 96-well non-treated flat-bottom sterile microtiter plates (Deltalab S.L., Spain) containing 100 μL of sufonamides at 0.1 mM (0.05 mM as a final concentration). Plates were incubated for 24 h at 37 °C. The OD_{620nm} was determined using the microtitre plate reader (Victor 3, PerkinElmer LAS, Waltham, MA, USA) to measure bacterial biomass. Supernatants were then aspirated and the plates were washed three times with distilled water. In order to fix the biofilm, plates were incubated at 65 °C for 15 min. The biofilm was stained by adding 200 μL of 0.1% crystal violet and the plates were incubated for 15 min at RT. The crystal violet was discarded and the plates were washed three times with distilled water. The plates were allowed to dry, incubating at 37 °C for at least 30 min. To dissolve the crystal violet, 250 μl of 30% acetic acid was added. Plates were incubated for 15 min at room temperature and 150 μL were transferred to a new plate and the OD_{550nm} was measured. At least two replicates per strain and condition were tested. Growth control wells containing bacteria in LB medium and control wells containing only sterile medium were included.

4.2.4. MIC determination

Minimal inhibitory concentrations (MIC) of colistin, was tested in accordance with Clinical and Laboratory Standards Institute and The European Committee on Antimicrobial Susceptibility Testing recommendations with some modifications [70,72]. Briefly, fresh log phase bacteria cultures were diluted in cation-adjusted Muller-Hinton Broth (cMHB) to a final concentration of 5 × 10^5 cfu/mL. Aliquots of 50 μl were added to each well of a 96-well plate containing 50 μl of 2-fold serial dilutions of colistin in duplicate and 100 μl of sulfonamides at 0.1 mM (from a stock solution at 10 mM dissolved in DMSO) to obtain a final concentration of 0.05 mM. Sterility (no bacteria) and growth (no antibiotic) controls were also prepared. Plates were incubated at 37 °C for 20 h. The optical density, was determined at 550 nm (OD_{550nm}) using a multilabel microtitre plate reader (Victor 3, PerkinElmer LAS, Waltham, MA, USA). MICs was determined as the antibiotic concentration that reduced ≥80% of bacterial growth compared with the positive control. At least two replicates per strain and condition were tested.

4.2.5. In vivo assays

Galleria mellonella larvae were used to evaluate the effect of sulfonamides after *S. maltophilia* infection as was previously described [34]. Briefly, At least 15 larvae with a weight of 300–400 mg and no signs of melanisation were infected with *S. maltophilia* K279a. Log-phase culture in LB medium was washed and adjusted with PBS to obtain 1 × 10^4 cfu per larva. Infective dose was confirmed by viable counts on LB agar plates. Larvae were infected injecting 5 μl of K7279a in the last proleg using a 50 μl- Hamilton® Microliter™ syringe. Infected larvae were incubated at 37 °C for 60 min. After incubation, larvae were incubated on ice for 15 min to anesthetise. 5 μl of PBS solution containing either DMSO (untreated group), colistin at final concentration of 0,5 μg/mL or sulfonamides at final concentration of 50 μM were injected in the last right proleg. The amounts of sulfonamides, colistin and DMSO injected were calculated as was previously described [64]. Larvae were incubated at 37 °C and the survival was recorded every 24 h. At least two replicates were made with different batches of larvae.

Declaration of competing interest

The authors declare that they have no known competing financial interests or personal relationships that could have appeared to influence the work reported in this paper.

Data availability

Data available in supplementary information

Acknowledgements

Conor Horgan is grateful for funding by way of a Government of Ireland Postgraduate Research Scholarship (GOIPG/2017/1111) provided by the Irish Research Council. Michelle O'Driscoll thanks the Irish Research Council for a Government of Ireland Postgraduate Research Scholarhsip (GOIPG/2021/227). Xavier Daura acknowledges funding from the Spanish MICINN (PID2019-111364RB-I00). Isidre Gibert acknowledges support from the Catalan AGAUR (2021 SGR00092).

Appendix A. Supplementary data

Supplementary data to this article can be found online at https://doi.org/10.1016/j.ejmech.2023.115819.

Abbreviations

ABA	*A. baumannii* ATCC 15308
BCC	Burkholderia cepacia complex
BCE	*B. cepacia* R6193
BCN	B. cenocepacia 289
BDSF	*Burkholderia* diffusible signal factor
BMU	B. multivorans B10
CoA	Coenzyme A
cMHB	Cation-adjusted Muller-Hinton Broth
CST	Colistin

DCC	*N*,*N*′-Dicyclohexylcarbodiimide
DCM	Dichloromethane
DMAP	Dimethylaminopyridine
DMF	Dimethylformamide
DMSO	Dimethyl sulfoxide
DSF	Diffusible signal factor
ECO	*E. coli* ATCC 9637
LB	Luria-Bertani
MIC	Minimal inhibitory concentration
MDR	Multidrug resistance
PAO	P. aeruginosa PAO1
PBS	Phosphate-buffered saline
QS	Quorum sensing
rpf	Regulation of pathogenicity factors
Sm	Stenotrophomonas maltophilia
SMA	S. maltophilia K279a
Xcc	*Xanthomonas campestris*

References

[1] Y. Deng, J. Wu, F. Tao, L.H. Zhang, Listening to a new language: DSF-based quorum sensing in Gram-negative bacteria, Chem. Rev. 111 (2011) 160–173.

[2] P.H. Williams, Black rot: a continuing threat to world crucifers, Plant Dis. 64 (1980) 736–742.

[3] J.L. Tang, Y.N. Liu, C.E. Barber, J.M. Dow, J.C. Wootton, M.J. Daniels, Genetic and molecular analysis of a cluster of rpf genes involved in positive regulation of synthesis of extracellular enzymes and polysaccharide in *Xanthomonas campestris pathovar campestris*, Mol. Gen. Genet. 226 (1991) 409–417.

[4] H. Slater, A. Alvarez-Morales, C.E. Barber, M.J. Daniels, J. Maxwell Dow, A two-component system involving an HD-GYP domain protein links cell-cell signalling to pathogenicity gene expression in *Xanthomonas campestris*, Mol. Microbiol. 38 (2000) 986–1003.

[5] L.H. Wang, Y. He, Y. Gao, J.E. Wu, Y.H. Dong, C. He, S.X. Wang, L.X. Weng, J.L. Xu, L. Tay, R.X. Fang, L.H. Zhang, A bacterial cell-cell communication signal with cross-kingdom structural analogues, Mol. Microbiol. 51 (2004) 903–912.

[6] C. Boon, Y.Y. Deng, L.H. Wang, Y.W. He, J.L. Xu, Y. Fan, S.Q. Pan, L.H. Zhang, A novel DSF-like signal from *Burkholderia cenocepacia* interferes with *Candida albicans* morphological transition, ISME J. 2 (2008) 27–36.

[7] E. Mahenthiralingam, A. Baldwin, P. Vandamme, *Burkholderia cepacia* complex infection in patients with cystic fibrosis, J. Med. Microbiol. 51 (2002) 533–538.

[8] H.J. Lo, J.R. Köhler, B. Didomenico, D. Loebenberg, A. Cacciapuoti, G.R. Fink, Nonfilamentous *C. albicans* mutants are avirulent, Cell 90 (1997) 939–949.

[9] D.G. Davies, C.N.H. Marques, A fatty acid messenger is responsible for inducing dispersion in microbial biofilms, J. Bacteriol. 191 (2009) 1393–1403.

[10] T.-P. Huang, A.C. Lee Wong, Extracellular fatty acids facilitate flagella-independent translocation by *Stenotrophomonas maltophilia*, Res. Microbiol. 158 (2007) 702–711.

[11] Y.-W. He, J.E. Wu, J.-S. Cha, L.-H. Zhang, Rice bacterial blight pathogen *Xanthomonas oryzae pv. oryzae* produces multiple DSF-family signals in regulation of virulence factor production, BMC Microbiol. 10 (2010) 1–9.

[12] M. Ionescu, K. Yokota, E. Antonova, A. Garcia, E. Beaulieu, T. Hayes, A.T. Iavarone, S.E. Lindow, Promiscuous diffusible signal factor production and responsiveness of the *Xylella fastidiosa* rpf system, mBio 7 (2016) 1–12.

[13] J.M. Dow, Diffusible signal factor-dependent quorum sensing in pathogenic bacteria and its exploitation for disease control, J. Appl. Microbiol. 122 (2017) 2–11.

[14] R.P. Ryan, J.M. Dow, Communication with a growing family: diffusible signal factor (DSF) signaling in bacteria, Trends Microbiol. 19 (2011) 145–152.

[15] P. Huedo, V.P. Kumar, C. Horgan, D. Yero, X. Daura, I. Gibert, T.P. O'Sullivan, Sulfonamide-based diffusible signal factor analogs interfere with quorum sensing in *Stenotrophomonas maltophilia* and *Burkholderia cepacia*, Future Med. Chem. 11 (2019) 1565–1582.

[16] S.-Q. An, J. Murtagh, K.B. Twomey, M.K. Gupta, T.P. O'Sullivan, R. Ingram, M. A. Valvano, J.-l. Tang, Modulation of antibiotic sensitivity and biofilm formation in *Pseudomonas aeruginosa* by interspecies signal analogues, Nat. Commun. 10 (2019) 2334.

[17] C. Ballatore, D.M. Huryn, A.B. Smith, Carboxylic acid (bio)isosteres in drug design, ChemMedChem 8 (2013) 385–395.

[18] N.A. Meanwell, Synopsis of some recent tactical application of bioisosteres in drug design, J. Med. Chem. 54 (2011) 2529–2591.

[19] C. Horgan, T.P. O'Sullivan, Recent developments in the practical application of novel carboxylic acid bioisosteres, Curr. Med. Chem. 29 (2022) 2203–2234.

[20] V.P. Kumar, M.K. Gupta, C. Horgan, T.P. O'Sullivan, Synthesis of the quorum sensing molecule Diffusible Signal Factor using the alkyne zipper reaction, Tetrahedron Lett. 59 (2018) 2193–2195.

[21] C. Dugave, L. Demange, *cis–trans* isomerization of organic molecules and biomolecules: implications and applications, Chem. Rev. 103 (2003) 2475–2532.

[22] T.P. O'Sullivan, K.S.A. Vallin, S.T.A. Shah, J. Fakhry, P. Maderna, M. Scannell, A.L. F. Sampaio, M. Perretti, C. Godson, P.J. Guiry, Aromatic lipoxin A4 and lipoxin B4 analogues display potent biological activities, J. Med. Chem. 50 (2007) 5894–5902.

[23] K. Daly, K. O'Sullivan, T.P. O'Sullivan, Major structure–activity relationships of resolvins, protectins, maresins and their analogues, Future Med. Chem. 14 (2022) 1943–1960.

[24] Y. Soltani, L.C. Wilkins, R.L. Melen, Stoichiometric and catalytic C–C and C–H bond formation with $B(C_6F_5)_3$ *via* cationic intermediates, Angew. Chem. Int. Ed. 56 (2017) 11995–11999.

[25] M. Larhed, C. Moberg, A. Hallberg, Microwave-accelerated homogeneous catalysis in organic chemistry, Acc. Chem. Res. 35 (2002) 717–727.

[26] P. Appukkuttan, E. Van der Eycken, Recent developments in microwave-assisted, transition-metal-catalysed C-C and C-N bond-forming reactions, 2008, Eur. J. Org. Chem. (2008) 1133–1155.

[27] M. Ghizzoni, J. Wu, T.L. Gao, H.J. Haisma, F.J. Dekker, 6-Alkylsalicylates are selective Tip60 inhibitors and target the acetyl-CoA binding site, Eur. J. Med. Chem. 47 (2012) 337–344.

[28] R. Chinchilla, C. Carmen Nájera, The Sonogashira reaction: a booming methodology in synthetic organic chemistry, Chem. Rev. 107 (2007) 874–922.

[29] F. Mohajer, M.M. Heravi, V. Zadsirjan, N. Poormohammad, Copper-free Sonogashira cross-coupling reactions: an overview, RSC Adv. 11 (2021) 6885–6925.

[30] T.T. Talele, The "cyclopropyl fragment" is a versatile player that frequently appears in preclinical/clinical drug molecules, J. Med. Chem. 59 (2016) 8712–8756.

[31] A.H. Ingall, J. Dixon, A. Bailey, M.E. Coombs, D. Cox, J.I. McInally, S.F. Hunt, N. D. Kindon, B.J. Teobald, P.A. Willis, R.G. Humphries, P. Leff, J.A. Clegg, J. A. Smith, W. Tomlinson, Antagonists of the platelet P2T receptor: a novel approach to antithrombotic therapy, J. Med. Chem. 42 (1999) 213–220.

[32] Y. McCarthy, L. Yang, K.B. Twomey, A. Sass, T. Tolker-Nielsen, E. Mahenthiralingam, J.M. Dow, R.P. Ryan, A sensor kinase recognizing the cell-cell signal BDSF (*cis*-2-dodecenoic acid) regulates virulence in *Burkholderia cenocepacia*, Mol. Microbiol. 77 (2010) 1220–1236.

[33] Y. Deng, A. Lim, J. Lee, S. Chen, S. An, Y.-H. Dong, L.-H. Zhang, Diffusible signal factor (DSF) quorum sensing signal and structurally related molecules enhance the antimicrobial efficacy of antibiotics against some bacterial pathogens, BMC Microbiol. 14 (2014) 1–9.

[34] A.-C. Gómez, T. Lyons, U. Mamat, D. Yero, M. Bravo, X. Daura, O. Elshafee, S. Brunke, C.G.M. Gahan, M. O'Driscoll, I. Gibert, T.P. O'Sullivan, Synthesis and evaluation of novel furanones as biofilm inhibitors in opportunistic human pathogens, Eur. J. Med. Chem. 242 (2022) 1–16.

[35] S. Navon-Venezia, R. Ben-Ami, Y. Carmeli, Update on *Pseudomonas aeruginosa* and *Acinetobacter baumannii* infections in the healthcare setting, Curr. Opin. Infect. Dis. 18 (2005) 306–313.

[36] D.L. Paterson, Serious infections in the intensive care unit: *Pseudomonas aeruginosa* and *Acinetobacter baumannii*, Clin. Infect. Dis. 43 (2006) S41–S42.

[37] D.M.P. De Oliveira, B.M. Forde, T.J. Kidd, P.N.A. Harris, M.A. Schembri, S. A. Beatson, D.L. Paterson, M.J. Walker, Antimicrobial resistance in ESKAPE pathogens, Clin. Microbiol. Rev. 33 (2020), e00181-00119.

[38] C. Harding, S. Hennon, M. Feldman, Uncovering the mechanisms of *Acinetobacter baumannii* virulence, Nat. Rev. Microbiol. 16 (2018) 91–102.

[39] M. Nicol, S. Alexandre, J.-B. Luizet, M. Skogman, T. Jouenne, S.P. Salcedo, E. Dé, Unsaturated fatty acids affect quorum sensing communication system and inhibit motility and biofilm formation of *Acinetobacter baumannii*, Int. J. Mol. Sci. 19 (2018) 214.

[40] A.L. Flores-Mireles, J.N. Walker, M. Caparon, S.J. Hultgren, Urinary tract infections: epidemiology, mechanisms of infection and treatment options, Nat. Rev. Microbiol. 13 (2015) 269–284.

[41] G. Sharma, S. Sharma, P. Sharma, D. Chandola, S. Dang, S. Gupta, R. Gabrani, *Escherichia coli* biofilm: development and therapeutic strategies, J. Appl. Microbiol. 121 (2016) 309–319.

[42] C.T. Archer, J.F. Kim, H. Jeong, J.H. Park, C.E. Vickers, S.Y. Lee, L.K. Nielsen, The genome sequence of *E. coli* W (ATCC 9637): comparative genome analysis and an improved genome-scale reconstruction of *E. coli*, BMC Genom. 12 (2011) 1–20.

[43] I.J. Abbott, A.Y. Peleg, *Stenotrophomonas, achromobacter*, and nonmelioid *Burkholderia* species: antimicrobial resistance and therapeutic strategies, Semin. Respir. Crit. Care Med. 36 (2015) 99–110.

[44] N. Rajkumari, P. Mathur, A.K. Gupta, K. Sharma, M.C. Misra, Epidemiology and outcomes of *Stenotrophomonas maltophilia* and *Burkholderia cepacia* infections among trauma patients of India: a five year experience, J. Infect. Prev. 16 (2015) 103–110.

[45] P.S. Ganesh, S. Vishnupriya, J. Vadivelu, V. Mariappan, K.M. Vellasamy, E. M. Shankar, Intracellular survival and innate immune evasion of *Burkholderia cepacia*: improved understanding of quorum sensing-controlled virulence factors, biofilm, and inhibitors, Microbiol. Immunol. 64 (2020) 87–98.

[46] M.M. Sfeir, *Burkholderia cepacia* complex infections: more complex than the bacterium name suggest, J. Infect. 77 (2018) 166–170.

[47] H. Wisplinghoff, *Pseudomonas spp.*, *acinetobacter spp.* and miscellaneous gram-negative bacilli, in: J. Cohen, W.G. Powderly, S.M. Opal (Eds.), Infectious Diseases, Elsevier, Amsterdam, 2017, pp. 1579–1599.

[48] A. Loutet Slade, A. Valvano Miguel, A decade of *Burkholderia cenocepacia* virulence determinant Research, Infect. Immun. 78 (2010) 4088–4100.

[49] A. Suppiger, N. Schmid, C. Aguilar, G. Pessi, L. Eberl, Two quorum sensing systems control biofilm formation and virulence in members of the *Burkholderia cepacia* complex, Virulence 4 (2013) 400–409.

[50] R. Reik, T. Spilker, J.J. Lipuma, Distribution of *Burkholderia cepacia* complex species among isolates recovered from persons with or without cystic fibrosis, J. Clin. Microbiol. 43 (2005) 2926–2928.
[51] J.F. Turton, M.E. Kaufmann, N. Mustafa, S. Kawa, F.E. Clode, T.L. Pitt, Molecular comparison of isolates of *Burkholderia multivorans* from patients with cystic fibrosis in the United Kingdom, J. Clin. Microbiol. 41 (2003) 5750–5754.
[52] N. Høiby, T. Bjarnsholt, M. Givskov, S. Molin, O. Ciofu, Antibiotic resistance of bacterial biofilms, Int. J. Antimicrob. Agents 35 (2010) 322–332.
[53] Y. Deng, C. Boon, S. Chen, A. Lim, L.-H. Zhang, *cis*-2-Dodecenoic acid signal modulates virulence of *Pseudomonas aeruginosa* through interference with quorum sensing systems and T3SS, BMC Microbiol. 13 (2013) 231.
[54] J. Klockgether, A. Munder, J. Neugebauer, F. Davenport Colin, F. Stanke, D. Larbig Karen, S.S. Heeb, U, M. Pohl Thomas, L. Wiehlmann, B. Tümmler, Genome diversity of *Pseudomonas aeruginosa* PAO1 laboratory strains, J. Bacteriol. 192 (2010) 1113–1121.
[55] J.S. Brooke, *Stenotrophomonas maltophilia*: an emerging global opportunistic pathogen, Clin. Microbiol. Rev. 25 (2012) 2–41.
[56] P. Huedo, X. Coves, X. Daura, I. Gibert, D. Yero, Quorum sensing signaling and quenching in the multidrug-resistant pathogen *Stenotrophomonas maltophilia*, Front. Cell. Infect. Microbiol. 8 (2018) 1–8.
[57] C.R. Hobby, J.L. Herndon, C.A. Morrow, R.E. Peters, S.J.K. Symes, D.K. Giles, Exogenous fatty acids alter phospholipid composition, membrane permeability, capacity for biofilm formation, and antimicrobial peptide susceptibility in *Klebsiella pneumoniae*, Microbiology Open 8 (2019), e00635.
[58] J.M. Schierholz, J. Beuth, G. Pulverer, Adherent bacteria and activity of antibiotics, J. Antimicrob. Chemother. 43 (1999) 158–160.
[59] K. LaPlante, J. Cusumano, G. Tillotson, Colistin for the treatment of multidrug-resistant infections, Lancet Infect. Dis. 18 (2018) 1174–1175.
[60] S. Martínez-Servat, D. Yero, P. Huedo, R. Marquez, G. Molina, X. Daura, I. Gibert, Heterogeneous colistin-resistance phenotypes coexisting in *Stenotrophomonas maltophilia* isolates influence colistin susceptibility testing, Front. Microbiol. 9 (2018) 1–10.
[61] J.H. Moffatt, M. Harper, P. Harrison, J.D.F. Hale, E. Vinogradov, T. Seemann, R. Henry, B. Crane, F. St Michael, A.D. Cox, B. Adler, R.L. Nation, J. Li, J.D. Boyce, Colistin resistance in *Acinetobacter baumannii* is mediated by complete loss of lipopolysaccharide production, Antimicrob. Agents Chemother. 54 (2010) 4971–4977.
[62] J.-Y. Lee, Y.K. Park, E.S. Chung, I.Y. Na, K.S. Ko, Evolved resistance to colistin and its loss due to genetic reversion in *Pseudomonas aeruginosa*, Sci. Rep. 6 (2016) 25543–25555.
[63] R.J. Malott, C.-H. Wu, T.D. Lee, T.J. Hird, N.F. Dalleska, J.E.A. Zlosnik, D. K. Newman, D.P. Speert, Fosmidomycin decreases membrane hopanoids and potentiates the effects of colistin on *Burkholderia multivorans* clinical isolates, Antimicrob. Agents Chemother. 58 (2014) 5211–5219.
[64] A. Andrea, K.A. Krogfelt, H. Jenssen, Methods and challenges of using the greater wax moth (*Galleria mellonella*) as a model organism in antimicrobial compound discovery, Microorganisms 7 (2019) 1–9.
[65] E. Allegra, R.W. Titball, J. Carter, O.L. Champion, *Galleria mellonella* larvae allow the discrimination of toxic and non-toxic chemicals, Chemosphere 198 (2018) 469–472.
[66] Y. López Hernández, D. Yero, J.M. Pinos-Rodríguez, I. Gibert, Animals devoid of pulmonary system as infection models in the study of lung bacterial pathogens, Front. Microbiol. 6 (2015) 1–19.
[67] A. Daina, O. Michielin, V. Zoete, SwissADME: a free web tool to evaluate pharmacokinetics, drug-likeness and medicinal chemistry friendliness of small molecules, Sci. Rep. 7 (2017) 1–13.
[68] T. Kitayama, Microbial asymmetric syntheses of 3-alkylphthalide derivatives, Tetrahedron: Asymmetry 8 (1997) 3765–3774.
[69] Clinical and Laboratory Standards Institute, in: Methods for Dilution Antimicrobial Susceptibility Tests for Bacteria that Grow Aerobically. Approved Standard, tenth ed., 2015.
[70] The European Committee on Antimicrobial Susceptibility Testing, Breakpoint Tables for Interpretation of MICs and Zone Diameters, 2018, Version 8.0.
[71] P. Huedo, D. Yero, S. Martínez-Servat, I. Estibariz, R. Planell, P. Martínez, A. Ruyra, N. Roher, I. Roca, J. Vila, X. Daura, I. Gibert, Two different *rpf* clusters distributed among a population of *Stenotrophomonas maltophilia* clinical strains display differential diffusible signal factor production and virulence regulation, J. Bacteriol. 196 (2014) 2431–2442.
[72] The European Committee on Antimicrobial Susceptibility Testing and Clinical and Laboratory Standards Institute, Recommendations for MIC Determination of Colistin (Polymyxin E) as Recommended by the Joint CLSI-EUCAST Polymyxin Breakpoints Working Group, 2016.